THE SMOLUCHOWSKI-POISSON-BOLTZMANN DESCRIPTION OF ION DIFFUSION AT CHARGED INTERFACES

DEREK Y. C. CHAN AND BERTIL HALLE
Department of Applied Mathematics, Research School of Physical Sciences, Australian National University, Canberra, ACT 2601, Australia

ABSTRACT A theoretical description of ion diffusion in the electric field set up by the double layer in the neighborhood of a charged interface is presented. Such a description is needed for the understanding of diffusion-controlled chemical kinetics and transport of ionic species in a variety of systems of interest in biophysics, electrochemistry, and colloid science. The ion dynamics are taken to be governed by the Smoluchowski diffusion equation and the average electrostatic field is obtained from the nonlinear Poisson-Boltzmann equation. Diffusion in finite regions with partially absorbing boundaries of planar, cylindrical, or spherical geometry is considered. The complete analytical solution of the Smoluchowski-Poisson-Boltzmann equation for counterions between two planar charged interfaces is given. Simple expressions are derived for certain useful integral quantities, viz., mean absorption times and absorption probabilities, in all geometries considered. Finally, lateral counterion diffusion and its consequences for surface re-encounter-enhanced chemoreception is considered.

INTRODUCTION

A wide range of problems in biophysics, electrochemistry, and colloid science relate to the properties of the electric double layer, consisting of an ionic solution in contact with a charged interface. Since the pioneering work of Gouy (1) and Chapman (2), a vast literature has accumulated concerning the derivation, accuracy, and application of the Poisson-Boltzmann (PB) equation and other theories of the equilibrium ion distribution in the double layer. In contrast, very little theoretical work has been devoted to ion diffusion in the double layer. However, such work is crucial to the understanding of diffusion-controlled chemical kinetics and transport of ionic species in an immense variety of systems. In dealing with these problems, previous authors have either resorted to linear approximations and numerical solutions (3, 4) or simply neglected many-body effects (screening) altogether (5, 6).

In the following, we present a number of simple analytic results of general validity related to ion diffusion in the electrical double layer, which can be derived without invoking any approximations beyond the nonlinear PB equation for the mean electrostatic potential and the Smoluchowski equation (7) for the diffusion of an ionic species in that potential. We consider diffusion in finite regions of space (as is always the case in practice), where the internal boundary consists of a charged interface of planar, cylindrical, or spherical geometry. Most of the results are strictly valid only for the no-salt case, i.e., when the ionic solution contains only the counterions required to balance the interfacial charge. However, for strongly overlapping double layers, the effect of the coions may be neglected (8) and our results should then provide reasonable approximations to the counterion dynamics in the presence of added salt.

The paper is organized as follows. First, we introduce some basic notation and briefly discuss the Smoluchowski-Poisson-Boltzmann (SPB) equation for the propagator $f(r, t|r_0)$. We then solve the SPB equation for the case of counterions between two charged planes to obtain the exact propagator in terms of elementary functions. Having obtained the most general solution, corresponding to partially absorbing boundaries at two arbitrarily located interior planes, we present, in Appendix A, the propagators for some useful special cases. With the aid of these propagators, one may investigate in detail the ion dynamics, for example, through the appropriate time correlation functions (B. Halle, manuscript in preparation).

In many applications, the full propagator is not needed and one requires only the probability that a given ion at time t has not yet reached a certain location or not yet become absorbed there. This probability can often be approximated by a decaying exponential with a characteristic mean absorption time (MAT). (We illustrate the accuracy of this exponential approximation for the planar case.) By direct integration of the PB equation, we obtain simple expressions for the MAT. For planar and cylindrical geometry, the results are analytical, whereas for spherical geometry, one integral remains to be evaluated numerically. Furthermore, we derive simple expressions for the

probability that an ion gets absorbed at one boundary rather than at the other one. The expressions for this probability, as well as for the MAT, are completely general in the sense that we allow for partial absorption at both boundaries.

Next follows a general discussion of the effects of geometry and potential on the MATs and on the absorption probability. We introduce a quasi-potential that enables us to express the Smoluchowski equation in a geometry-independent form. It is seen that the effect of geometry is equivalent to that of a logarithmic potential. We also comment briefly on the form equivalence between surface and space diffusion for certain geometries.

Finally, we study the extent of lateral vs. radial ion diffusion in the electrical double layer. This question is closely related to the concept of reduction of dimensionality for diffusion in finite regions as advanced by Adam and Delbrück (9). However, as emphasized by Berg and Purcell (10), even in the absence of physical adsorption, a diffusing ligand executes a quasi–two-dimensional random walk in the vicinity of the interface for extended periods of time. This intriguing phenomenon, which leads to a highly efficient sampling of the interface by the ligand, may be regarded as a special case of the well-known effect of reactant-pair re-encounters on the kinetics of homogenous solution reactions (12), viz., the case where the reactant partners differ greatly in size. We present simple expressions for the mean number of ion-surface encounters and for the surface coverage of absorbing receptor sites needed to achieve a given ultimate absorption probability. We show that the electrostatic interactions in the double layer may enhance the re-encounter effect by several orders of magnitude. This result should be of considerable interest in biological as well as technological applications involving chemoreception (6, 10) or heterogeneous catalysis at charged interfaces (cells, organelles, macromolecules, surfactant micelles, etc.).

THE SPB EQUATION

We shall consider ion diffusion in a finite three-dimensional space bounded by two surfaces, one of which is charged (see Fig. 1). Such a diffusion space will be called a cell. A parameter s specifies the cell geometry: planar ($s = 1$), cylindrical ($s = 2$), or spherical ($s = 3$). The coordinate perpendicular to the boundaries will be called the radial coordinate, r. The radii of the charged interface and the outer cell boundary are denoted by a and b, respectively. (In the planar case, there is only one relevant length scale and we may set $a \equiv 0$.) Note that the planar case emerges from the other two geometries in the limit $a, b \gg (b - a)$.

The planar cell may represent an actual structural element, such as a synaptic cleft or part of a multibilayer structure (liposome, lyotropic mesophase). The cylindrical and spherical cells may represent, to a good approximation, the average structure of an isotropic solution, the solute

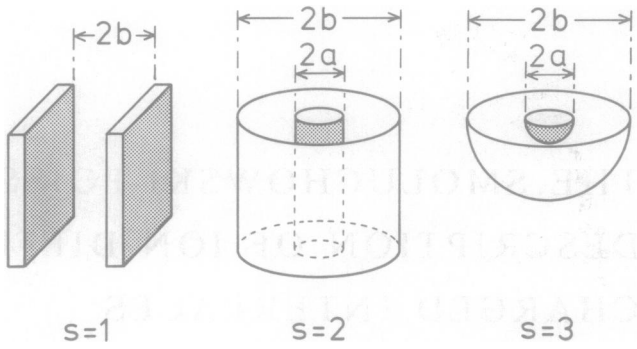

FIGURE 1 Geometry of the diffusion cell. Charged surfaces have been shaded. The planar ($s = 1$) and cylindrical ($s = 2$) geometries are treated as effectively infinite in two and one dimension(s), respectively.

concentration of which is related to the cell radius b. For $s = 2$,

$$b = (\pi l n_m)^{-1/2}, \tag{1a}$$

where l is the length of the cylinder unit that carries one elementary charge and n_m is the number density of such units (monomers in the case of a linear polyelectrolyte). For $s = 3$,

$$b = \left(\frac{4}{3}\pi n_c\right)^{-1/3}, \tag{1b}$$

where n_c is the number density of spherical solutes, e.g., protein molecules or surfactant micelles.

As usual, we model the ionic solution as a collection of point charges, ze, imbedded in a homogeneous dielectric of relative permittivity ϵ_r. The interficial charge distribution is represented by a fixed uniform surface charge density, σ. This surface charge is balanced by an opposite net charge in the ionic solution, so that the entire cell is electroneutral. Because of the radial symmetry of the boundaries and the fixed surface charge distribution, the mean electrostatic potential, $\psi(r)$, averaged over the position of all ions, must also be radially symmetric.

If, in addition to the approximations inherent in the description of the interactions, one introduces a statistical-mechanical mean-field approximation, one obtains the PB equation for the mean electrostatic potential, $\psi(r)$. For a radially symmetric system with no added salt, i.e., with only counterions in the ionic solution, the PB equation is

$$r^{1-s}\frac{d}{dr}[r^{s-1}\psi'(r)] = -\frac{zen(b)}{\epsilon_0\epsilon_r}\exp\left[-\frac{ze\psi(r)}{k_BT}\right], \tag{2}$$

where the prime denotes differentiation with respect to r and $n(r) \equiv n(b)\exp[-ze\psi(r)/k_BT]$ is the local counterion number density. At the outer cell boundary, $\psi(b) \equiv 0$ by convention. Because of the electroneutrality of the cell, we have the boundary conditions

$$\psi'(a) = -\frac{\sigma}{\epsilon_0\epsilon_r} \tag{3a}$$

and

$$\psi'(b) = 0. \tag{3b}$$

If the surface potential ψ_0 is given, rather than the surface charge density σ, then Eq. 3a is replaced by

$$\psi(a) = \psi_0. \tag{3c}$$

Analytical solutions to Eq. 2 exist for planar and cylindrical geometry (12–14). For spherical geometry, however, one must resort to numerical methods.

While the potential obtained by solving Eq. 2 is strictly valid only for the no-salt case, it does remain accurate even in the presence of added salt as long as $|ze\psi(r)| \gg k_BT$ for all r, so that the coions contribute negligibly to the double-layer charge distribution (8). All the results in this paper that are based on the no-salt PB Eq. 2 are therefore valid also in the presence of salt as long as this so-called strong overlap condition is satisfied.

All information about the ion self-diffusion process is contained in the propagator $f(\vec{r}, t|\vec{r}_0)$. Because of the radial symmetry of $\psi(r)$, we shall be concerned only with the radial propagator $f(r, t|r_0)$, which is obtained by integrating over the other two coordinates. The quantity $f(r, t|r_0)r^{s-1}dr$ is the probability of finding a given ion in a "shell" of thickness dr around r at time t, given that it had the radial coordinate r_0 initially. (We choose to define $f(r, t|r_0)$ so as to incorporate the angular factors of $2\pi[s = 2]$ and $4\pi(s = 3)$.) We shall assume that the radial propagator satisfies the Smoluchowski mean-field diffusion equation (7)

$$\frac{\partial}{\partial t}f(r,t|r_0) = r^{1-s}\frac{\partial}{\partial r}r^{s-1}D(r)\left[\frac{\partial}{\partial r} + \phi'(r)\right]f(r,t|r_0). \tag{4}$$

In some of the following sections, we shall allow for a spatial dependence in the counterion diffusion coefficient $D(r)$; this may account for dynamical correlations with solvent molecules (15, 16). However, in most applications, one will have a constant D, which will then act merely to scale the time coordinate. In Eq. 4, $\phi(r)$ is the potential of mean force acting on the diffusing particle, expressed in units of k_BT. We shall approximate $\phi(r)$ by the (reduced) mean PB potential,

$$\phi(r) = \frac{ze\psi(r)}{k_BT}, \tag{5}$$

which is obtained by solving Eq. 2. When this approximation has been made, we shall refer to Eq. 4 as the Smoluchowski-Poisson-Boltzmann (SPB) equation.

In order to solve the partial differential Eq. 4, we need an initial condition and two boundary conditions. The former is

$$f(r, 0|r_0) = r^{1-s}\delta(r - r_0). \tag{6}$$

The boundary conditions are expressed in terms of the radial flux density, $j(r, t|r_0)$, which is related to the propagator through the continuity equation

$$\frac{\partial}{\partial t}f(r,t|r_0) + r^{1-s}\frac{\partial}{\partial r}r^{s-1}j(r,t|r_0) = 0. \tag{7}$$

Comparison with Eq. 4 shows that

$$j(r,t|r_0) = -D(r)\left[\frac{\partial}{\partial r} + \phi'(r)\right]f(r,t|r_0), \tag{8a}$$

which can also be expressed as

$$j(r,t|r_0) = -D(r)e^{-\phi(r)}\frac{\partial}{\partial r}[e^{\phi(r)}f(r,t|r_0)]. \tag{8b}$$

The most general boundary condition is the partial absorption (or "radiation") condition

$$j(a,t|r_0) + a^{1-s}\kappa_a f(a,t|r_0) = 0, \tag{9a}$$

$$j(b,t|r_0) - b^{1-s}\kappa_b f(b,t|r_0) = 0, \tag{9b}$$

where the coefficients κ_a and κ_b measure the absorption efficiency at each boundary. For example, with $r = a$ perfectly reflecting and $r = b$ perfectly absorbing, we have $\kappa_a = 0$ and $\kappa_b = \infty$. If both boundaries are perfectly reflecting, then $f(r, t|r_0)$ evolves toward the equilibrium distribution

$$f(r) = e^{-\phi(r)}\left[\int_a^b dr\, r^{s-1}\, e^{-\phi(r)}\right]^{-1}. \tag{10}$$

However, if κ_a or κ_b is finite, then $f(r, \infty|r_0) = 0$.

In many applications in chemical kinetics (11, 17, 18), the diffusing particle may either decay spontaneously (e.g., electronic deactivation) or react with another species (usually called the scavenger). The effects of a spontaneous decay or of a uniform scavenger distribution can be incorporated simply by adding to the right-hand side of the Smoluchowski Eq. 4 a sink term $-k_1 f(r, t|r_0)$, where k_1 is a first-order (or pseudo–first-order) rate constant. As can easily be verified, the propagator then becomes

$$f(r, t|r_0; k_1) = e^{-k_1 t}\, f(r, t|r_0; k_1 = 0). \tag{11}$$

COUNTERION DIFFUSION IN PLANAR GEOMETRY

In this section, we shall present an analytic solution to the SPB equation for planar geometry and partially absorbing boundaries. We consider the diffusion of a counterion within an arbitrary "slice" ($c_1 \le r \le c_2$) of the space between two charged planes (see Fig. 2). The midplane is at $r = 0$ and the charged planes are at $r = \pm b$. (When considering single-cell diffusion spaces elsewhere in this paper, we take $r = a$ or 0 at the charged interface and $r = b$ at the outer cell boundary, which is the midplane in the planar case.)

The solution to Eq. 2 with $s = 1$ that satisfies the

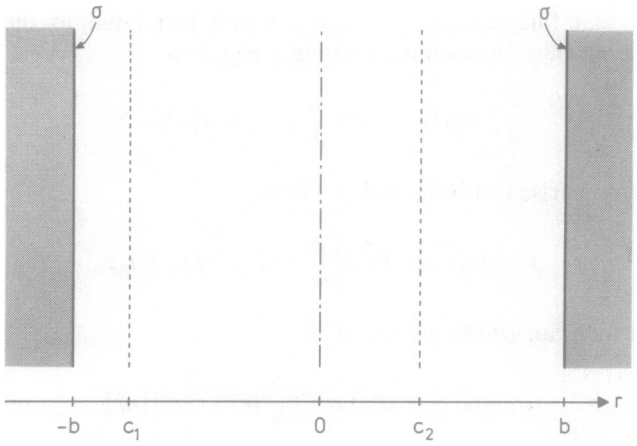

FIGURE 2 The charged planes are located at $r = \pm b$. The diffusing counterion is confined to the range $c_1 \le r \le c_2$, with $-b \le c_1 < c_2 \le b$.

boundary conditions of Eq. 3 is (12, 14)

$$\phi(\xi) \equiv \frac{ze\psi(\xi)}{k_B T} = 2 \ln \cos \xi, \tag{12}$$

where we have introduced the dimensionless coordinate

$$\xi \equiv \kappa r = \gamma x. \tag{13}$$

The reciprocal Debye length, κ, is defined by

$$\kappa \equiv \left[\frac{z^2 e^2 n(0)}{2\epsilon_0 \epsilon_r k_B T}\right]^{1/2}. \tag{14}$$

Furthermore,

$$\gamma \equiv \kappa b \tag{15}$$

and

$$x \equiv \frac{r}{b}. \tag{16}$$

Since the counterion density at the midplane, $n(0)$, is unknown, we need an additional relation to determine κ or γ. This relation is obtained by substituting Eq. 12 into either of the boundary conditions of Eqs. 3a and 3c. The result is

$$\gamma \tan \gamma = \frac{|ze\sigma| b}{2\epsilon_0 \epsilon_r k_B T} \tag{17a}$$

or

$$\gamma = \arccos \exp\left(\frac{ze\psi_0}{2k_B T}\right). \tag{17b}$$

When solving the transcendental Eq. 17*a*, care must be taken to choose, among the infinity of solutions, the one in the interval $[0, \pi/2]$. For convenience, this solution is plotted in Fig. 3, from which it is also seen that the

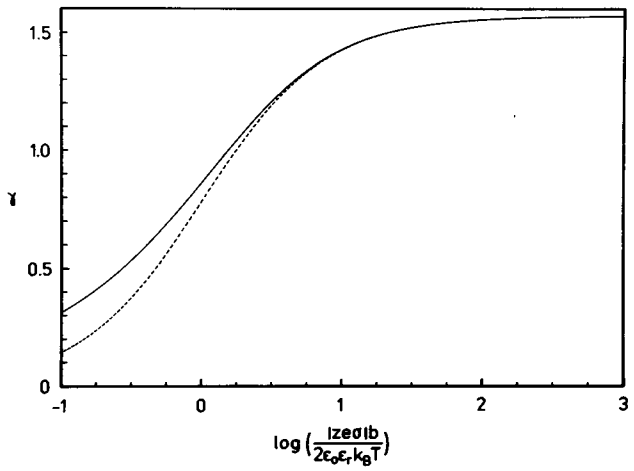

FIGURE 3 The solution to the transcendental Eq. 17a (solid curve). The approximate Eq. 18 (dashed curve) is accurate to better than 1% for $\gamma \gtrsim 1.2$.

approximation

$$\gamma \approx \frac{\pi}{2}\left(1 + \frac{2\epsilon_0 \epsilon_r k_B T}{|ze\sigma| b}\right)^{-1} \tag{18}$$

is quite accurate in the strong coupling regime.

If, in Eq. 4, we set $s = 1$, let D be a constant, introduce the dimensionless time variable

$$\tau \equiv \kappa^2 D t = \gamma^2 \frac{Dt}{b^2} \tag{19}$$

and the dimensionless propagator

$$\tilde{f}(\xi, \tau | \xi_0) \equiv \frac{b}{\gamma} f(\xi, \tau | \xi_0), \tag{20}$$

and make use of Eqs. 12 and 13, we get the SPB equation

$$\frac{\partial}{\partial \tau} \tilde{f}(\xi, \tau | \xi_0) = \frac{\partial}{\partial \xi}\left[\frac{\partial}{\partial \xi} - 2 \tan \xi\right] \tilde{f}(\xi, \tau | \xi_0). \tag{21}$$

The general solution to the Smoluchowski diffusion equation can always be written as an eigenfunction expansion (19), which in the case of Eq. 21 takes the form

$$\tilde{f}(\xi; \tau | \xi_0) = \frac{\cos \xi_0}{\cos \xi} \sum_{n=0}^{\infty} \frac{y_n(\xi_0) y_n(\xi)}{N_n} \exp\left[-(\lambda_n^2 - 1)\tau\right]. \tag{22}$$

The derivation of the eigenfunctions $y_n(\xi)$, the eigenvalues λ_n, and the normalization constants N_n, which depend on the form of the potential and on the boundary conditions, can be found in Appendix A. Also included there are some useful special cases of the general solution.

As defined in Appendix A, the quantities $(\lambda_n^2 - 1)$ are nonzero positive numbers. Consequently, the propagator $\tilde{f}(\xi; \tau | \xi_0)$ decays to zero as $\tau \to \infty$. However, in the special case that both boundaries are perfectly reflecting, the propagator should decay, not to zero, but to the equilib-

rium distribution $\tilde{f}(\xi)$. In this case, we must therefore add to the right-hand side of Eq. 22

$$\tilde{f}(\xi) = \frac{\sec^2\xi}{\tan\xi_2 - \tan\xi_1}, \tag{23}$$

where $\xi_i \equiv \kappa c_i = \gamma c_i/b$. This equilibrium distribution, which was obtained from Eqs. 10 and 12, is normalized according to

$$\int_{\xi_1}^{\xi_2} d\xi \tilde{f}(\xi) = 1. \tag{24}$$

The propagator given by Eq. 22 and Appendix A completely determines the self-diffusion of counterions in a system with planar geometry and the most general boundary conditions. But its usefulness extends beyond applications to planar geometry since, by virtue of its analyticity, it reveals, in a qualitative way, many features of the (radial) counterion diffusion in other geometries. (The cylindrical and spherical cases, in particular, reduce to the planar case whenever $a, b \gg b - a$.)

A quantity of interest in many applications is the probability, $Q(t)$, that a given counterion has not yet been absorbed at one of the boundaries at time τ. It is obtained from the propagator by averaging the initial position over the equilibrium distribution and integrating the current position over the entire diffusion space, i.e.,

$$Q(\tau) = \int_{\xi_1}^{\xi_2} d\xi_0 \tilde{f}(\xi_0) \int_{\xi_1}^{\xi_2} d\xi \tilde{f}(\xi, \tau | \xi_0). \tag{25}$$

As will be shown in the next section, the mean time that elapses before the particle is absorbed is (in units of $b^2[\gamma^2 D]^{-1}$).

$$\tau_{abs} = \int_0^\infty d\tau\, Q(\tau). \tag{26}$$

In order to exhibit the simplicity of the results, we end this section by giving explicit formulae for $Q(\tau)$ and τ_{abs} in the special case that the charged interface is perfectly reflecting, while the midplane is perfectly absorbing. From Appendix A, we have

$$Q(\tau) = 2\gamma \cot\gamma \sum_{n=0}^{\infty} \left\{\left[(2n+1)\frac{\pi}{2}\right]^2 - \gamma^2\right\}^{-1} \cdot \exp\left[-\left\{\left[(2n+1)\frac{\pi}{2}\right]^2 - \gamma^2\right\}\frac{\tau}{\gamma^2}\right]. \tag{27}$$

Inserting this into Eq. 26 and performing the integration, we get

$$\tau_{abs} = 2\gamma^3 \cot\gamma \sum_{n=0}^{\infty} \left\{\left[(2n+1)\frac{\pi}{2}\right]^2 - \gamma^2\right\}^{-2}, \tag{28}$$

which can be summed exactly (20) to give

$$\tau_{abs} = \frac{\gamma}{2}\left(\tan\gamma + \cot\gamma - \frac{1}{\gamma}\right). \tag{29}$$

In the next section, we show how this simple result can be derived more directly.

In the strong coupling regime, when the right-hand side of Eq. 17a greatly exceeds unity, γ approaches its maximum value of $\pi/2$. The decay of $Q(\tau)$ is then completely dominated by the slow decay of the first term in the sum of Eq. 27. It is easy to show that the time constant of this slowly decaying exponential approaches τ_{abs}, which is essentially given by the first term in Eq. 28. Hence, in the strong coupling limit,

$$Q(\tau) \approx \exp\left(-\frac{\tau}{\tau_{abs}}\right). \tag{30}$$

In Fig. 4 we illustrate the accuracy of this approximation in two cases: no coupling ($\gamma = 0$), i.e., free diffusion, and a

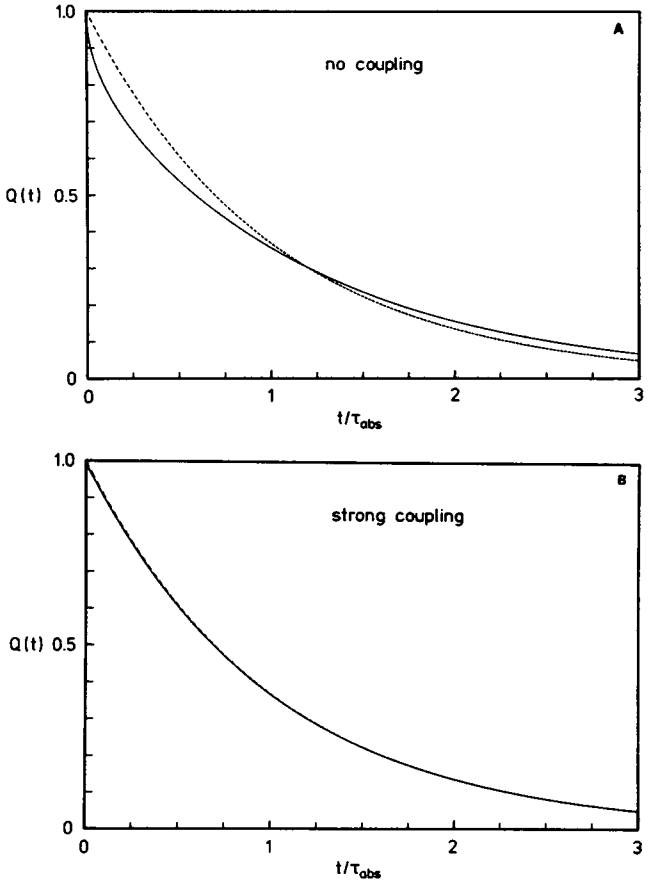

FIGURE 4 The probability, $Q(t)$, that a diffusing particle remains, at time t, in a planar system with a charged reflecting boundary ($r = -b$ in Fig. 2) and an absorbing cell boundary ($r = 0$). Solid curves represent the exact Eq. 27 and dashed curves represent the exponential approximation in Eq. 30. The mean absorption time, τ_{abs}, is (in units of b^2/D) 1/3 for free diffusion ($\gamma = 0$) and 20.47 for the strong coupling example ($\gamma = 1.555245$, $C/\lambda = 100$, $\phi_0 = -8.3273$).

strong coupling example ($\gamma = 1.555245$). Because of the close agreement between the exponential approximation, Eq. 30, and the exact result, Eq. 27, it is, for many purposes, sufficient to characterize the diffusion process by a suitably defined MAT. In the following section, we therefore present expressions for MATs of counterions diffusing in an electric double layer.

THE MAT FOR ARBITRARY POTENTIAL

The first-passage time concept has been widely used in the dynamical description of physical processes (21). When applied to translational diffusion, as done first by Schrödinger (22) and von Smoluchowski (23), the mean first-passage time, τ, gives the mean time taken for a diffusing particle to reach a given coordinate for the first time. For free diffusion in an infinite (or semi-infinite) one-dimensional space,

$$\tau = \frac{x^2}{2D}, \tag{31}$$

which can be regarded as the converse of the famous Einstein-Smoluchowski relation for the mean-square displacement $\langle x^2 \rangle$, accumulated during a given period of time

$$\langle x^2 \rangle = 2Dt. \tag{32}$$

As was first shown by Pontrjagin et al. (24, 24a) (see also references 17 and 25–27), the mean first-passage time for a particle diffusing in a bounded one-dimensional system in the presence of an external field can be expressed as a convoluted double integral involving the Boltzmann factor of the external potential. This result is important because it circumvents the need to solve the Smoluchowski equation to get the propagator and to then perform the infinite sum, as we did in deriving Eq. 29. When the external field has radial symmetry, the extension to cylindrical or spherical boundaries is straightforward (26). While most interest has been focused on perfectly absorbing or perfectly reflecting boundaries, it is possible to generalize the result of Pontrjagin et al. (24, 24a) to partially absorbing boundaries (28, 29). In the presence of partially absorbing boundaries, one asks for the mean time required for a diffusing particle to become absorbed at some point. Since absorption does not necessarily occur at the first visit, we shall henceforth use the term mean absorption time (MAT) rather than mean first-passage time.

In this section, we present the general MAT formulae for radially symmetric systems with arbitrary external potential of mean force and with partially absorbing boundaries. These formulae have appeared in the literature before; however, most of them were in a less general form. In the following section, we shall focus on the PB double-layer potential and show how, in that case, the general formulae lead to simple expressions for the MAT. In particular, we shall show that the MAT can be expressed in terms of a single integral, without the need to evaluate the convoluted double integral. For planar and cylindrical geometry, this single integral can be performed analytically.

The probability that a given particle, which was located at $r = r_0$ initially, has not yet been absorbed at time t is obtained by integrating the propagator over the diffusion space, i.e.,

$$Q(t \mid r_0) = \int_a^b dr\, r^{s-1} f(r, t \mid r_0). \tag{33}$$

Obviously, $Q(0 \mid r_0) = 1$ and, unless both boundaries are perfectly reflecting, $Q(\infty \mid r_0) = 0$. The absorption probability density, $F(t \mid r_0)$, where $F(t \mid r_0)dt$ is the probability that the particle is absorbed between t and $t + dt$, is given by

$$F(t \mid r_0) = b^{s-1} j(b, t \mid r_0) - a^{s-1} j(a, t \mid r_0) = -\frac{\partial Q(t \mid r_0)}{\partial t}. \tag{34}$$

The second equality can be verified by integrating the continuity equation, Eq. 7, over the diffusion space and then using Eq. 33. The MAT $\tau(r_0)$ is the mean time that is required for a particle, initially located at $r = r_0$, to become absorbed at a boundary; i.e.,

$$\tau(r_0) = \int_0^\infty dt\, t\, F(t \mid r_0) = \int_0^\infty dt\, Q(t \mid r_0), \tag{35}$$

where the second equality follows from Eq. 34 and integration by parts. We shall indicate the nature of the boundaries by two subscripts on $\tau(r_0)$: A for perfectly absorbing, R for perfectly reflecting, and P for partially absorbing. The first subscript refers to the inner boundary ($r = a$) and the second subscript refers to the outer boundary ($r = b$).

The general expression for $\tau_{pp}(r_0)$ can be derived from the Smoluchowski equation, Eq. 4, and Eq. 35 with the boundary conditions of Eq. 9. Several different derivations have been presented in the literature, the simplest being the direct integration method of Deutch (29). The result is

$$\tau_{pp}(r_0) = \frac{1 + \kappa_a f(a) J_1(a, r_0) + \kappa_b f(b) \bar{J}_1(r_0, b) + \kappa_a \kappa_b f(a) f(b) [J_0 J_1(a, r_0) - J_0(a, r_0) J_1]}{\kappa_a f(a) + \kappa_b f(b) + \kappa_a \kappa_b f(a) f(b) J_0}. \tag{36}$$

Here we have introduced the integrals

$$J_n(r_1, r_2) \equiv \int_{r_1}^{r_2} dr\, [D(r) r^{s-1} f(r)]^{-1} \left[\int_r^b dr' r'^{s-1} f(r') \right]^n, \tag{37a}$$

$$\bar{J}_n(r_1, r_2) \equiv \int_{r_1}^{r_2} dr\, [D(r) r^{s-1} f(r)]^{-1} \left[\int_a^r dr' r'^{s-1} f(r') \right]^n. \tag{37b}$$

The equilibrium distribution $f(r)$ is defined in Eq. 10. Whenever $r_1 = a$ and $r_2 = b$, we shall, as in Eq. 36, omit the arguments of J_n and $\bar{J}_n$. These integrals are interrelated

through

$$J_1(r_1, r_2) + \bar{J}_1(r_1, r_2) = J_0(r_1, r_2) = \bar{J}_0(r_1, r_2), \quad (38a)$$

$$J_2 - J_1 = \bar{J}_2 - \bar{J}_1. \quad (38b)$$

The rather formidable-looking Eq. 36 simplifies considerably in important special cases. Thus, if $r = a$ is perfectly reflecting ($\kappa_a = 0$),

$$\tau_{RP}(r_0) = [\kappa_b f(b)]^{-1} + \bar{J}_1(r_0, b); \quad (39a)$$

if $r = b$ is perfectly reflecting ($\kappa_b = 0$),

$$\tau_{PR}(r_0) = [\kappa_a f(a)]^{-1} + J_1(a, r_0); \quad (39b)$$

and, if both boundaries are perfectly absorbing ($\kappa_a = \kappa_b = \infty$),

$$\tau_{AA}(r_0) = \frac{J_0 J_1(a, r_0) - J_0(a, r_0) J_1}{J_0}. \quad (39c)$$

Another quantity of interest is the MAT, τ_{pp}, corresponding to an initial equilibrium distribution. It is obtained by averaging $\tau_{pp}(r_0)$ over $f(r_0)$, i.e.,

$$\tau_{pp} = \int_a^b dr_0\, r_0^{s-1} f(r_0)\, \tau_{pp}(r_0). \quad (40)$$

With Eqs. 36 and 37, this leads to

$$\tau_{pp} = \frac{1 + \kappa_a f(a) J_2 + \kappa_b f(b) \bar{J}_2 + \kappa_a \kappa_b f(a) f(b) [J_0 J_2 - J_1^2]}{\kappa_a f(a) + \kappa_b f(b) + \kappa_a \kappa_b f(a) f(b) J_0}. \quad (41)$$

An expression equivalent to Eq. 41 was derived by Deutch (29). From Eq. 41, we obtain the special cases

$$\tau_{RP} = [\kappa_b f(b)]^{-1} + \bar{J}_2; \quad (42a)$$

$$\tau_{PR} = [\kappa_a f(a)]^{-1} + J_2; \quad (42b)$$

$$\tau_{AA} = \frac{J_0 J_2 - J_1^2}{J_0}. \quad (42c)$$

From the above it follows also that

$$\tau_{RP}(a) - \tau_{RP} = \tau_{PR}(b) - \tau_{PR}. \quad (43)$$

In the foregoing, we have tacitly assumed that absorption can take place only at the boundaries $r = a$ and/or $r = b$. But we might also want to know, for example, the mean time, $\tau_{RA}(r_0 \to c)$, required for a particle initially at $r = r_0$ to reach $r = c$ for the first time, when $a \leq r_0 < c < b$. (The subscript R now refers to $r = a$ and A to $r = c$. Since the particle is absorbed at $r = c$, we do not have to specify the nature of the $r = b$ boundary.) We then set $b = c$ in the preceding formulae, so that, according to Eq. 39*a*, $\tau_{RA}(r_0 \to c) = \bar{J}_1(r_0, c)$. If, as in the no-salt double-layer case, the external potential depend explicitly on b, then $\tau_{RA}(r_0 \to c)$ will, of course, also depend on b, albeit not via the integration limits.

It is sometimes convenient to define an excess MAT by subtracting off the corresponding free-diffusion MAT. The excess MAT is particularly useful if it can be defined in such a way that it becomes independent of b. For example, from Eqs. 37b and 39a, we have the excess MAT

$$\Delta\tau_{RA}(r_0) = \int_{r_0}^b dr\, [D(r) r^{s-1} f(r)]^{-1} \int_a^r dr' r'^{s-1} f(r') - \int_{r_0}^b dr\, [D(r) r^{s-1}]^{-1} \int_a^r dr' r'^{s-1}. \quad (44)$$

A b-independent excess MAT can be obtained in the limit

$$\Delta\tau_{RA}^{\infty}(r_0) \equiv \lim_{b \to \infty} \Delta\tau_{RA}(r_0). \quad (45)$$

This quantity is a measure of the maximum effect of the potential on the MAT. If $f(r)$ is independent of b and if $D(r)$ approaches a constant value for large r, then it can be shown that $\Delta\tau_{RA}^{\infty}(r_0)$ diverges as b for planar geometry ($s = 1$) and as $\ln b$ for cylindrical geometry ($s = 2$). However, for spherical geometry ($s = 3$), $\Delta\tau_{RA}^{\infty}(r_0)$ is finite, provided that $\phi(r)$ decays faster than r^{-2}. With a constant diffusion coefficient, we get, for $s = 3$,

$$D\Delta\tau_{RA}^{\infty}(r_0) = \frac{1}{r_0} \int_a^{r_0} dr\, r^2 [e^{-\phi(r)} - 1] + \int_{r_0}^{\infty} dr\, r [e^{-\phi(r)} - 1] + \int_{r_0}^{\infty} dr\, r^{-2} \cdot [e^{\phi(r)} - 1] \int_a^r dr'\, r'^2 [e^{-\phi(r')} - 1] + \frac{1}{3} \int_{r_0}^{\infty} dr (r - a^3 r^{-2}) [e^{\phi(r)} - 1]. \quad (46)$$

THE MAT FOR THE PB POTENTIAL

We shall now apply the formulae of the preceding section to the case of a z-valent counterion diffusing among other identical counterions (but no coions) in the ionic solution outside a charged interface (located at $r = a$) of planar ($s = 1$), cylindrical ($s = 2$), or spherical ($s = 3$) geometry. The potential of mean force acting upon a counterion is approximated by the mean electrostatic potential as given by the PB equation, Eq. 2, with the boundary conditions of Eq. 3. In dimensionless form, we have

$$\frac{d}{dx} [x^{s-1} \phi'(x)] = -2\gamma^2 x^{s-1} e^{-\phi(x)}; \quad (47a)$$

$$\phi'(\lambda) = \frac{2C}{\lambda}; \quad (47b)$$

$$\phi'(1) = \phi(1) = 0, \quad (47c)$$

where ϕ, γ, and x are defined by Eqs. 5, 15, and 16, respectively, and where we have introduced the further dimensionless quantities

$$\lambda \equiv \frac{a}{b} \quad (48a)$$

$$C \equiv \frac{|ze\sigma|a}{2\epsilon_0\epsilon_r k_B T}. \tag{48b}$$

Using Eqs. 10 and 47, we can now express the convoluted multiple integrals of Eq. 37 in a simple form, where only the following integral remains to be evaluated:

$$I_s(x_1, x_2) \equiv \int_{x_1}^{x_2} dx\, x^{1-s}\, e^{\phi(x)}. \tag{49}$$

Considering the relationships of Eq. 38, we need only evaluate three integrals, viz.,

$$J_0(x_1, x_2) = \frac{b^2}{D\gamma^2}\lambda^{s-2} C\, I_s(x_1, x_2); \tag{50a}$$

$$J_1(x_1, x_2) = \frac{b^2}{2D\gamma^2}[e^{\phi(x_2)} - e^{\phi(x_1)}]; \tag{50b}$$

$$J_2 = \frac{b^2}{2D\gamma^2}[\gamma^2(1-\lambda^s)/s - e^{\phi(\lambda)}], \tag{50c}$$

where we have assumed a constant diffusion coefficient.

Combination of Eqs. 10, 36, 38, and 50 now leads to

$$\tau_{PP}(x_0) = \frac{b^s\lambda^{s-2}C}{K_s\gamma^2} + \frac{b^2}{2D\gamma^2}\left[e^{\phi(x_0)} + \frac{1}{K_s}[2\kappa_b\lambda^{s-2}C\, I_s(x_0, 1) - \kappa_a - \kappa_b] + \frac{\kappa_a\kappa_b b^{2-s}}{DK_s}e^{-\phi(\lambda)}\{[1 - e^{\phi(\lambda)}]\, I_s(x_0, 1) - I_s\}\right], \tag{51}$$

where

$$K_s \equiv \kappa_a\, e^{-\phi(\lambda)} + \kappa_b + \kappa_a\kappa_b\, e^{-\phi(\lambda)}\, b^{2-s}\, I_s/D. \tag{52}$$

In the special cases, Eq. 51 reduces to

$$\tau_{RP}(x_0) = \frac{b^s\lambda^{s-2}C}{\kappa_b\gamma^2} + \frac{b^2}{2D\gamma^2}\{2\lambda^{s-2}CI_s(x_0, 1) - [1 - e^{\phi(x_0)}]\}; \tag{53a}$$

$$\tau_{PR}(x_0) = \frac{b^s\lambda^{s-2}C}{\kappa_a\gamma^2}e^{\phi(\lambda)} + \frac{b^2}{2D\gamma^2}[e^{\phi(x_0)} - e^{\phi(\lambda)}]; \tag{53b}$$

$$\tau_{AA}(x_0) = \frac{b^2}{2D\gamma^2}\{[1 - e^{\phi(\lambda)}]I_s(x_0, 1)/I_s - [1 - e^{\phi(x_0)}]\}. \tag{53c}$$

In a similar way, we obtain from Eqs. 10, 38, 41, and 51:

$$\tau_{PP} = \frac{b^s\lambda^{s-2}C}{K_s\gamma^2} + \frac{b^2}{D}\left\{\frac{(1-\lambda^s)}{2s\lambda^{s-2}C} - \frac{e^{\phi(\lambda)}}{2\gamma^2} - \frac{\kappa_b}{K_s\gamma^2}[1 - e^{\phi(\lambda)} - \lambda^{s-2}CI_s] - \frac{\kappa_a\kappa_b b^{2-s}e^{-\phi(\lambda)}\,[1 - e^{\phi(\lambda)}]^2}{4D\gamma^{s-2}CK_s\gamma^2}\right\}, \tag{54}$$

with the special cases

$$\tau_{RP} = \frac{b^s\lambda^{s-2}C}{\kappa_b\gamma^2} + \frac{b^2}{D}\left\{\frac{(1-\lambda^s)}{2s\lambda^{s-2}C} - \frac{1}{\gamma^2}[1 - \frac{1}{2}e^{\phi(\lambda)} - \lambda^{s-2}CI_s]\right\}; \tag{55a}$$

$$\tau_{PR} = \frac{b^s\lambda^{s-2}C}{\kappa_a\gamma^2}e^{\phi(\lambda)} + \frac{b^2}{D}\left[\frac{(1-\lambda^s)}{2s\lambda^{s-2}C} - \frac{e^{\phi(\lambda)}}{2\gamma^2}\right]; \tag{55b}$$

$$\tau_{AA} = \frac{b^2}{D}\left\{\frac{(1-\lambda^s)}{2s\lambda^{s-2}C} - \frac{e^{\phi(\lambda)}}{2\gamma^2} - \frac{[1 - e^{\phi(\lambda)}]^2}{4\lambda^{s-2}CI_s\gamma^2}\right\}. \tag{55c}$$

In the limit of vanishing coupling ($C = 0$, $\gamma = 0$), the preceding MAT formulae for double-layer counterion diffusion reduce to those for free diffusion. However, the free-diffusion results are more directly obtained by setting $\phi(r) \equiv 0$ in Eq. 10 and substituting the result into Eqs. 36, 37, and 41. Assuming a constant diffusion coefficient and transforming to the dimensionless radial coordinate $x = r/b$, we get

$$\tau_{PP}(x_0) = \frac{b^s(1-\lambda^s)}{sK_s} + \frac{b^2}{sD}\left\{\frac{1}{2}(\lambda^2 - x_0^2) + \frac{1}{K_s}[\kappa_a I_s + \frac{\kappa_b}{2}(1-\lambda^2) - (\kappa_a + \lambda^s\kappa_b)I_s(x_0, 1) + \frac{\kappa_a\kappa_b}{2D}b^{2-s}(1-\lambda^2)I_s(\lambda, x_0)]\right\} \tag{56}$$

and

$$\tau_{PP} = \frac{b^s(1-\lambda^s)}{sK_s} + \frac{b^2}{sD(1-\lambda^s)}\left\{\frac{(1-\lambda^{s+2})}{(s+2)} + \frac{1}{K_s}[(\kappa_a + \lambda^{2s}\kappa_b)I_s - (\kappa_a + \lambda^s\kappa_b)(1-\lambda^2) - \frac{\kappa_a\kappa_b}{4D}b^{2-s}(1-\lambda^2)^2]\right\}, \tag{57}$$

where

$$K_s \equiv \kappa_a + \kappa_b + \kappa_a\kappa_b\, b^{2-s}I_s/D \tag{58}$$

and

$$I_s(x_1, x_2) \equiv \int_{x_1}^{x_2} dx\, x^{1-s} = \begin{cases} x_2 - x_1, & s = 1; \\ \ln(x_2/x_1), & s = 2; \\ \dfrac{1}{x_1} - \dfrac{1}{x_2}, & s = 3. \end{cases} \tag{59}$$

Special cases of Eqs. 56 and 57 have appeared frequently in the literature (6, 9, 10, 25, 28).

For planar and cylindrical geometry, the PB Eq. 47 has an analytic solution and the integral $I_s(x_1, x_2)$ in Eq. 49 is elementary. Some explicit results are given in Appendix B (planar geometry) and in Appendix C (cylindrical geometry). For the planar case, Figs. 5–7 display the magnitudes of several MATs. Note that the MATs (expressed in units of b^2/D) in Figs. 5 and 6 are completely determined by the coupling parameter C/λ (see Eq. 48).

In connection with Figs. 5 and 6, it is instructive to consider the shape of the PB mean potential (Eq. 12) in the strong coupling regime, where $C/\lambda \gg 1$ and γ approaches $\pi/2$ (see Eq. 17*a* and Fig. 3). In this coupling regime, the potential falls very sharply near the charged interface, while it remains quite flat in the neighborhood of the cell

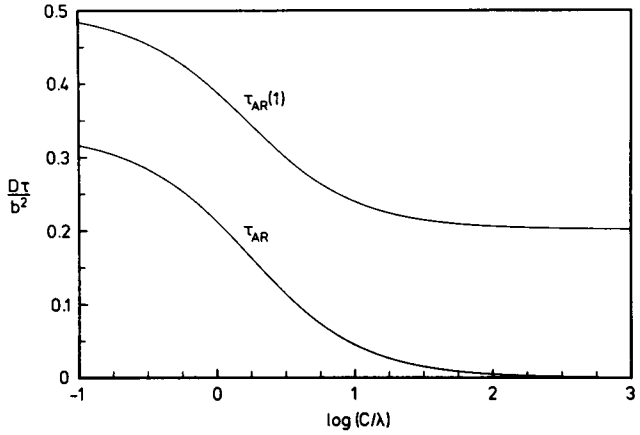

FIGURE 5 MATs for inward (toward the charged interface) diffusion in planar geometry vs. the coupling parameter $C/\lambda = |ze\sigma|b\ (2\epsilon_0\epsilon_r k_B T)^{-1}$. In the free-diffusion limit ($C/\lambda = 0$), $D\tau_{AR}(1)/b^2 = 1/2$, and $D\tau_{AR}/b^2 = 1/3$.

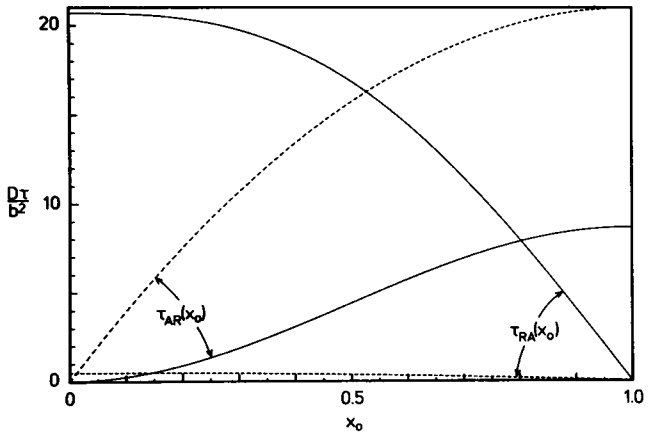

FIGURE 7 MATs in planar geometry vs. initial position x_0 (in units of b). The two τ_{AR} (x_0) curves have been scaled up by a factor of 42; e.g., $\tau_{AR}(1) = \tau_{RA}(0) = 1/2$ for free diffusion. Solid curves are examples of strong coupling ($\gamma = 1.555245$, $C/\lambda = 100$, $\phi_0 = -8.33$), while dashed curves represent free diffusion ($\gamma = 0$).

boundary. The behavior of the MATs for diffusion toward the charged interface (Fig. 5) can now be rationalized. As the coupling becomes stronger, τ_{AR} tends to zero because most initial positions are very close to the charged interface, whereas $\tau_{AR}(1)$ levels off at a constant value $[D\tau_{AR}(1)/b^2 = 2/\pi^2]$, which reflects the nearly free diffusion in the neighborhood of the cell boundary.

As for diffusion away from the charged interface, Fig. 6 shows that, in the strong coupling regime, $\tau_{RA} \approx \tau_{RA}(0)$, since most initial positions are near the charged interface ($x = 0$). Moreover, in this regime, $D\tau_{RA}/b^2 = 2C/(\pi^2\lambda)$, i.e., the MAT is proportional to b^3. It is seen that the mean residence time of a counterion in the double layer can be several orders of magnitude longer than if it were governed (Fig. 7) by free diffusion.

For planar geometry, it is of interest also to consider the counterion diffusion in the entire interlamellar space, rather than just in the region on either side of the midplane. The preceding analysis is readily extended, and in Fig. 8 we show the mean time for diffusion from one of the charged interfaces to an arbitrary coordinate x. The expression for this MAT is given by Eq. B12. It is noteworthy that, in the strong coupling example, counterions make considerable excursions from the charged interface ($x = -1$) on a relatively short time scale, even though they have to diffuse against a very strong electrostatic force. From Fig. 8 we can thus deduce that, for $C/\lambda = 100$, $b = 10$ nm, and $D = 1 \times 10^{-9}$ m^2 s^{-1}, it takes 4 μs to diffuse across the interlamellar space, whereas a mere 0.2 μs is required to diffuse from the interface, where $\phi = -8.33$, to a point 4 nm out, where $\phi = -1$. The long residence time of a counterion in the double layer is thus not due to a continuous long-time confinement in the deep potential well in the immediate neighborhood of the charged interface, but is rather a cumulative "Sisyphus effect" with the

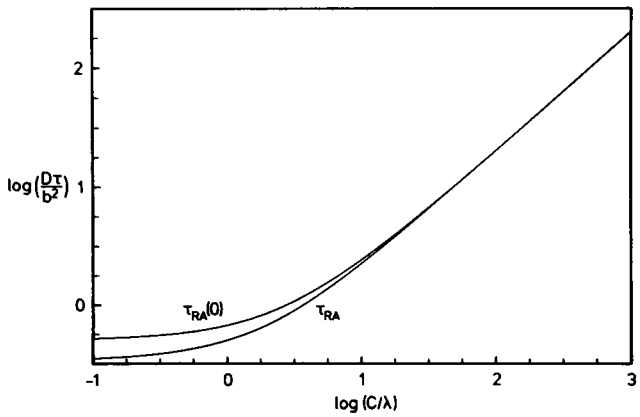

FIGURE 6 MATs for outward diffusion in planar geometry vs. the coupling parameter $C/\lambda = |ze\sigma|b\ (2\epsilon_0\epsilon_r k_B T)^{-1}$. In the free-diffusion limit ($C/\lambda = 0$), $D\tau_{RA}(0)/b^2 = 1/2$, and $D\tau_{RA}/b^2 = 1/3$.

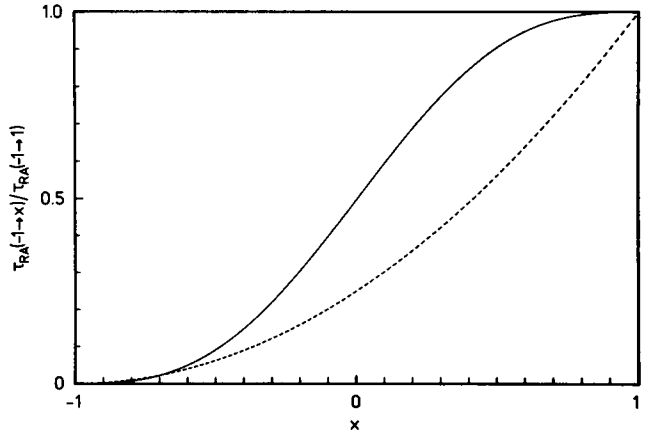

FIGURE 8 The mean time, τ_{RA} ($-1 \to x$), for diffusion from the left interface to the coordinate x, in units of τ_{RA} ($-1 \to 1$). The solid curve is an example of strong coupling [$\gamma = 1.555245$, $C/\lambda = 100$, $\phi_0 = -8.33$, $D\tau_{RA}$ ($-1 \to 1$)$/b^2 = 41.76$], while the dashed curve represents free diffusion [$\gamma = 0$, $D\tau_{RA}$ ($-1 \to 1$)$/b^2 = 2$].

counterion repeatedly "falling" back into the well after nearly having escaped from the double layer (cf. the discussion of surface re-encounters).

In this connection, we note a general property of the MAT τ_{RA} $(-1 \rightarrow 1)$ for diffusion across the interlamellar region (the interfaces of which are now located at $x = \pm 1$). According to Eq. 39a,

$$\tau_{RA}(-1 \rightarrow 1) = \bar{J}_1(-1, 1). \tag{60}$$

Now, for any potential that is symmetric with respect to the midplane, i.e., for which

$$\phi(-x) = \phi(x), \tag{61}$$

it follows from Eq. 37 (with $s = 1$ and constant D) that

$$\bar{J}_1(-1, 1) = 2[\bar{J}_1(-1, 0) + J_1(-1, 0)], \tag{62}$$

where the integrals on the right-hand side refer to a half-lamella. Combination of Eqs. 39, 60, and 62 then yields

$$\tau_{RA}(-1 \rightarrow 1) = 2[\tau_{RA}(0) + \tau_{AR}(1)], \tag{63}$$

where the MATs on the right-hand side refer to a half-lamella (with reflection or absorption at the midplane $x = 1$). In the strong coupling regime, the right-hand side of Eq. 63 is dominated by one of the MATs [τ_{RA} (0) if the diffusing particle is attracted to the interfaces] and the mean time taken to cross the interlamellar space is just twice the mean time required to diffuse, against the field, from the interface to the midplane or vice versa. By contrast, in the free-diffusion case it takes, on the average, four times as long to traverse the interlamellar space as to diffuse from interface to midplane. These general predictions are borne out by Fig. 8.

In the planar case, the dimensionless MATs $D\tau/b^2$ are determined completely by the single parameter C/λ. For cylindrical or spherical geometry, however, the MATs depend on two parameters: the coupling parameter C (independent of the cell size b) and the cell size parameter λ (independent of the coupling). MAT plots for cylindrical and spherical geometry are shown in Figs. 9–12. The qualitative behavior in cylindrical geometry is reminiscent of that in planar geometry. For example, Fig. 9 shows the leveling off of $\tau_{AR}(1)$ in the strong coupling regime [if also $\lambda \rightarrow 0$, then $D\tau_{AR}(1)/b^2 = 1/2$], while Fig. 10 shows that, in the strong coupling regime, τ_{RA} (λ) is proportional to the coupling parameter C [if also $\lambda \rightarrow 0$, then $D\tau_{RA}(\lambda)/b^2 = (5C - 2)/4$]. A difference between planar and cylindrical geometry is that in the latter the "target" for inward diffusion vanishes in the limit $\lambda \rightarrow 0$. As a consequence, $D\tau_{AR}(1)/b^2$ for free diffusion diverges in the limit of infinite dilution. However, as the electrostatic coupling increases ($C > 1$), this geometric effect is canceled and $D\tau_{AR}(1)/b^2$ attains a finite value even for $\lambda \rightarrow 0$ (see Fig. 9).

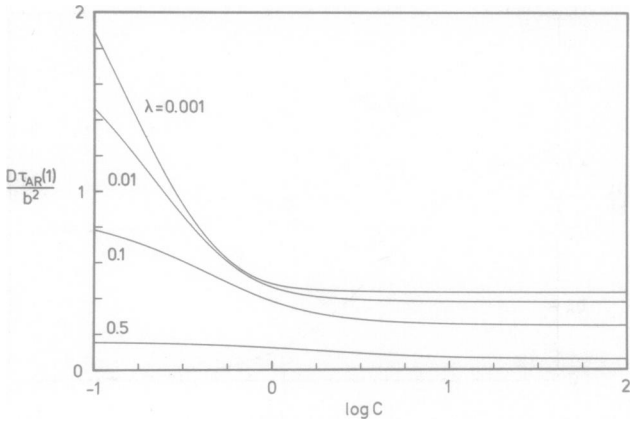

FIGURE 9 MAT for inward diffusion in cylindrical geometry vs. the coupling parameter $C = |ze\sigma|a\,(2\epsilon_0\epsilon_r k_B T)^{-1}$ for different values of the cell size parameter $\lambda = a/b$. In the free-diffusion limit ($C = 0$), $D\tau_{RA}(1)/b^2 = 0.16$, 0.90, 2.05, and 3.20 in order of decreasing λ.

The simple asymptotic behavior exhibited by the MATs for cylindrical geometry is not apparent in Figs. 11 and 12 for spherical geometry. It can be seen that as $\lambda \rightarrow 0$ at fixed coupling, the MATs approach the free-diffusion limit. Thus, $D\tau_{AR}(1)/b^2$ diverges, while $D\tau_{RA}(\lambda)/b^2 \rightarrow 1/6$. As C increases at fixed $\lambda \ll 1$, the onset of electrostatic retardation of the outward diffusion occurs abruptly at a critical C value.

In this section, we have obtained MAT expressions for the no-salt PB potential. As noted above, these results remain approximately valid in the presence of added salt in the strong overlap regime. In the opposite regime of weak overlap, i.e., thin double layers (8), an excess MAT for spherical geometry can be obtained from Eq. 46. In the general case, the free-diffusion and no-salt results given here provide lower and upper bounds for counterion MATs and absorption probabilities.

ABSORPTION PROBABILITIES

In this section, we consider the probability $P_{PP}(a|r_0)$ [and its complement $P_{PP}(b|r_0)$] that a given particle, which is known to be located at $r = r_0$ at some instant, eventually gets absorbed at the $r = a$ boundary rather than at the $r = b$ boundary. The nature of the boundaries is indicated by subscripts as for the MAT. (Here, however, the cases with one or two perfectly reflecting boundaries are trivial.) Unless both boundaries are perfectly reflecting, the particle is certain to get absorbed eventually, so that

$$P_{PP}(a|r_0) + P_{PP}(b|r_0) = 1. \tag{64}$$

In the limit $b \rightarrow \infty$, $P_{PP}(a|r_0)$ and $P_{PP}(b|r_0)$ are usually referred to as the capture and escape probabilities, respectively.

A differential equation satisfied by the escape probability (for arbitrary geometry) has been derived by Onsager (30) and Tachiya (31) and later extended to partial absorption by Sano and Tachiya (32). If there is radial

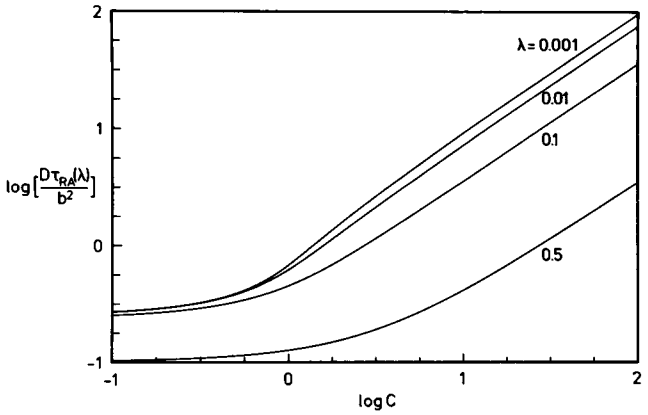

FIGURE 10 MAT for outward diffusion in cylindrical geometry vs. the coupling parameter $C = |ze\sigma|a\,(2\epsilon_0\epsilon_r k_B T)^{-1}$ for different values of the cell size parameter $\lambda = a/b$. In the free-diffusion limit ($C = 0$), $D\tau_{RA}(\lambda)/b^2 = 0.10, 0.24, 0.25$, and 0.25 in order of decreasing λ.

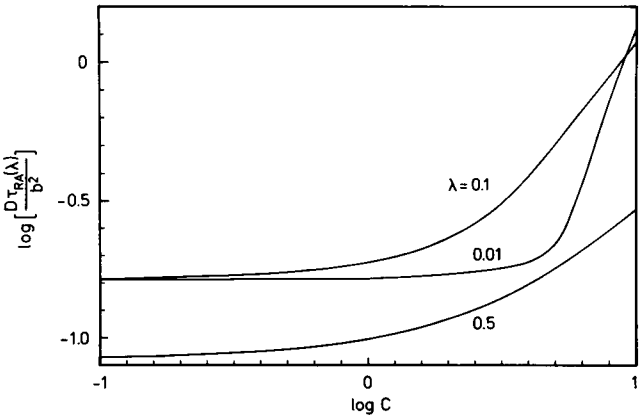

FIGURE 12 MAT for outward diffusion in spherical geometry vs. the coupling parameter $C = |ze\sigma|a\,(2\epsilon_0\epsilon_r k_B T)^{-1}$ for different values of the cell size parameter $\lambda = a/b$. In the free-diffusion limit ($C = 0$), $D\tau_{RA}(\lambda)/b^2 = 0.083, 0.16$, and 0.17 in order of decreasing λ.

symmetry, the solution to this differential equation can be expressed in terms of the integrals defined by Eq. 37. This solution can, however, also be obtained by the direct integration method used by Deutch (29) for the MAT. The general result, which is derived by this simple method in Appendix D, is

$$P_{PP}(a|r_0) = \frac{\kappa_a f(a) + \kappa_a\kappa_b f(a) f(b) J_0(r_0, b)}{\kappa_a f(a) + \kappa_b f(b) + \kappa_a\kappa_b f(a) f(b) J_0}; \quad (65a)$$

$$P_{PP}(b|r_0) = \frac{\kappa_b f(b) + \kappa_a\kappa_b f(a) f(b) J_0(a, r_0)}{\kappa_a f(a) + \kappa_b f(b) + \kappa_a\kappa_b f(a) f(b) J_0}. \quad (65b)$$

Special cases of Eq. 65 have appeared in the literature (17, 27, 30, 31, 33).

The absorption probability with initial equilibrium distribution is given by

$$P_{PP}(a) = \int_a^b dr_0\, r_0^{s-1} f(r_0)\, P_{PP}(a|r_0) \quad (66)$$

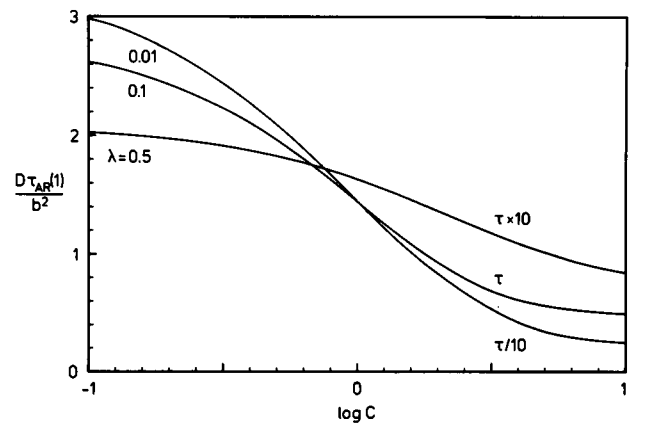

FIGURE 11 MAT for inward diffusion in spherical geometry vs. the coupling parameter $C = |ze\sigma|a\,(2\epsilon_0\epsilon_r k_B T)^{-1}$ for different values of the cell size parameter $\lambda = a/b$. Note that the curves are scaled differently. In the free-diffusion limit ($C = 0$), $D\tau_{AR}(1)/b^2 = 0.21$, 2.84, and 32.8 in order of decreasing λ.

and similarly for $P_{PP}(b)$. With Eqs. 37 and 65, this leads to

$$P_{PP}(a) = \frac{\kappa_a f(a) + \kappa_a\kappa_b f(a) f(b) \bar{J}_1}{\kappa_a f(a) + \kappa_b f(b) + \kappa_a\kappa_b f(a) f(b) J_0}; \quad (67a)$$

$$P_{PP}(b) = \frac{\kappa_b f(b) + \kappa_a\kappa_b f(a) f(b) J_1}{\kappa_a f(a) + \kappa_b f(b) + \kappa_a\kappa_b f(a) f(b) J_0}. \quad (67b)$$

The extension of Eqs. 65 and 67 to internal absorbing boundaries is straightforward, as already discussed for the MAT. For example, the probability that a particle, which is known to be at $r = r_0$ at some instant, reaches $r = c_1$ before $r = c_2$ (with $c_1 < r_0 < c_2$) is given by Eq. 65a as

$$P_{AA}(c_1, c_2|r_0) = \frac{J_0(r_0, c_2)}{J_0(c_1, c_2)}. \quad (68)$$

It is possible to express the general MAT formula, Eq. 36, in terms of the absorption probabilities. Using Eqs. 36–39 and 65, we find

$$\tau_{PP}(r_0) = \tau_{RP}(r_0) - P_{PP}(a|r_0)\tau_{RP}(a) = \tau_{PR}(r_0) - P_{PP}(b|r_0)\tau_{PR}(b). \quad (69)$$

Special cases of Eq. 69 have appeared in the literature (27, 34).

The absorption probabilities for double-layer counterion diffusion are obtained by combining Eqs. 10, 38, 50, 65, and 67 to give (with $x \equiv r/b$)

$$P_{PP}(\lambda|x_0) = \frac{\kappa_a}{K_s} e^{-\phi(\lambda)}\left[1 + \kappa_b \frac{b^{2-s}}{D} I_s(x_0, 1)\right]; \quad (70a)$$

$$P_{PP}(1|x_0) = \frac{\kappa_b}{K_s}\left[1 + \kappa_a e^{-\phi(\lambda)} \frac{b^{2-s}}{D} I_s(\lambda, x_0)\right]; \quad (70b)$$

$$P_{PP}(\lambda) = \frac{\kappa_a}{K_s} e^{-\phi(\lambda)}\left\{1 + \kappa_b \frac{b^{2-s}}{D}\left[I_s - \frac{(1 - e^{\phi(\lambda)})}{2\lambda^{s-2} C}\right]\right\}; \quad (71a)$$

$$P_{PP}(1) = \frac{\kappa_b}{K_s}\left\{1 + \frac{\kappa_a b^{2-s}}{2D\lambda^{s-2}C}\left[e^{-\phi(\lambda)} - 1\right]\right\}; \qquad (71b)$$

with the special cases

$$P_{AA}(\lambda \mid x_0) = \frac{I_s(x_0, 1)}{I_s}; \qquad (72a)$$

$$P_{AA}(\lambda) = 1 - \frac{[1 - e^{\phi(\lambda)}]}{2\lambda^{s-2}CI_s}. \qquad (72b)$$

The free-diffusion limit is recovered by setting $\phi \equiv 0$ in Eq. 70 or in Eqs. 10, 37, and 67. For example, one obtains the following capture probabilities ($b \to \infty$)

$$P_{PA}(a \mid r_0) = 1 \qquad (s = 1 \text{ or } 2); \qquad (73a)$$

$$P_{PA}(a \mid r_0) = \frac{1}{r_0}\left(\frac{D}{\kappa_a} + \frac{1}{a}\right)^{-1} \qquad (s = 3). \qquad (73b)$$

The certainty of capture in planar ($s = 1$) and cylindrical ($s = 2$) geometry was first pointed out by Pólya (35). For a perfectly absorbing boundary at $r = a$, Eq. 73*b* reduces to the familiar result

$$P_{AA}(a \mid r_0) = \frac{a}{r_0} \qquad (s = 3). \qquad (73c)$$

Again, we obtain analytic expressions for the absorption probabilities of counterions diffusing in planar and cylindrical geometry. Some of these formulae are given in Appendices B and C. Figs. 13–15 show the absorption probability vs. initial position for the three geometries, in each case for a strong coupling example and for free diffusion. The effect of the geometry of the diffusion space on the absorption probability is discussed in the next section. The symmetry in Fig. 13 is a manifestation of a general result for diffusion between two planar boundaries

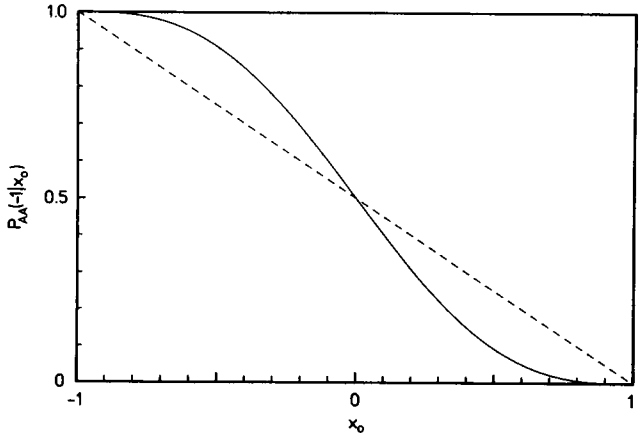

FIGURE 13 The probability, $P_{AA}(-1 \mid x_0)$, that a counterion located at x_0 and confined by charged planar interfaces at $x = \pm 1$, reaches the left interface ($x = -1$) before it reaches the right one. The solid curve is an example of strong coupling ($\gamma = 1.555245$, $C/\lambda = 100$, $\phi_0 = -8.33$), while the dashed line represents free diffusion ($\gamma = 0$).

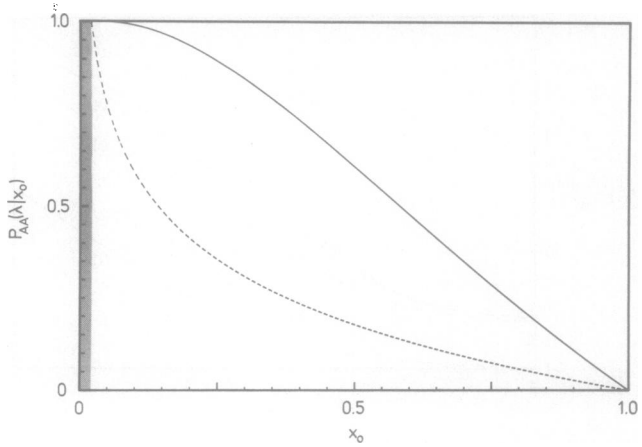

FIGURE 14 The probability, $P_{AA}(\lambda \mid x_0)$, that a counterion, located at x_0 in a cylindrical cell, reaches the charged interface ($x = \lambda$) before it reaches the cell boundary ($x = 1$). The solid curve is an example of strong coupling ($C = 5$, $\lambda = 0.02$, $\phi_0 = -10.29$), while the dashed curve represents free diffusion ($C = 0$, $\lambda = 0.02$).

with a potential that is symmetric with respect to the midplane. From Eq. 65a,

$$P_{AA}(-1 \mid x_0) = \frac{J_0(x_0, 1)}{J_0(-1, 1)}. \qquad (74)$$

According to Eqs. 37 and 61,

$$J_0(-x_0, 1) + J_0(x_0, 1) = J_0(-1, 1), \qquad (75)$$

so that

$$P_{AA}(-1 \mid -x_0) + P_{AA}(-1 \mid x_0) = 1. \qquad (76)$$

EFFECTS OF GEOMETRY AND POTENTIAL

For the purpose of discussing the effects of the geometry of the diffusion space, it is convenient to write the Smoluchowski equation in dimensionless form. With $x \equiv r/b$ and

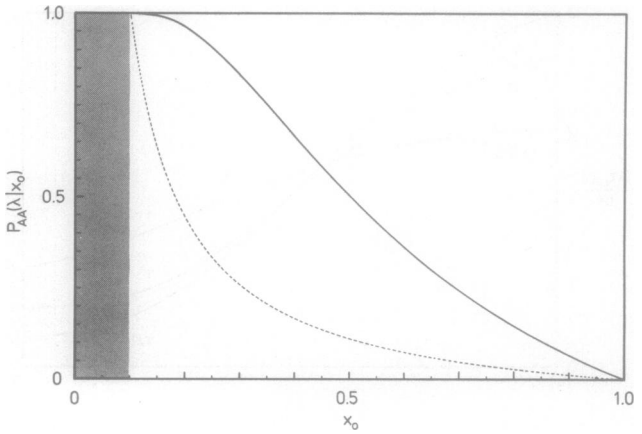

FIGURE 15 The probability, $P_{AA}(\lambda \mid x_0)$, that a counterion, located at x_0 in a spherical cell, reaches the charged interface ($x = \lambda$) before it reaches the cell boundary ($x = 1$). The solid curve is an example of strong coupling ($C = 10$, $\lambda = 0.1$, $\phi_0 = -8.64$), while the dashed curve represents free diffusion ($C = 0$, $\lambda = 0.1$).

$\tau \equiv Dt/b^2$, Eq. 4 reads

$$\frac{\partial}{\partial \tau} f(x, \tau \mid x_0) = x^{1-s} \frac{\partial}{\partial x} x^{s-1} \cdot \left[\frac{\partial}{\partial x} f(x, \tau \mid x_0) + \phi'(x) f(x, \tau \mid x_0) \right], \quad (77)$$

where we have assumed a constant diffusion coefficient.

Consider first the case of free diffusion [$\phi'(x) \equiv 0$] between perfectly reflecting or absorbing boundaries (κ_a, $\kappa_b = 0$ or ∞). From Eq. 77 and the boundary conditions of Eq. 9, it then follows immediately that the MATs can be expressed as

$$(\tau_{RA}, \tau_{AR}, \tau_{AA}) = \frac{b^2}{D} F_s(\lambda), \quad (78)$$

where F_s is a geometry-dependent function of $\lambda = a/b$. This observation was central to the discussion of biological diffusion processes by Adam and Delbrück (9). We emphasize that Eq. 78 is valid for all values of λ.

In the presence of a spatially varying potential $\phi(x)$, Eq. 78 is not generally valid. This is because $\phi(x)$ may depend on a or b separately, rather than on their ratio. This is the case for the PB potential in the absence of added electrolyte. As an example, consider planar geometry. From Eqs. 17a and B1, it is clear that $\phi(x)$ depends explicitly on b (for constant surface charge density). Indeed, it follows from Eqs. B8 and B9 that in the limit of very strong coupling ($\gamma \approx \pi/2$),

$$\tau_{RA} \propto b^3; \quad (79a)$$

$$\tau_{AR} \propto b. \quad (79b)$$

Some insight about the effect of a spatially varying potential, $\phi(x)$, on the diffusion may be gained by defining a propagator

$$g(x, \tau \mid x_0) \equiv x^{s-1} f(x, \tau \mid x_0) \quad (80)$$

and a quasi-potential

$$\tilde{\phi}(x) \equiv \phi(x) - (s - 1) \ln x. \quad (81)$$

In terms of these quantities, Eq. 77 becomes

$$\frac{\partial}{\partial \tau} g(x, \tau \mid x_0) = \frac{\partial^2}{\partial x^2} g(x, \tau \mid x_0) + \frac{\partial}{\partial x} [\tilde{\phi}'(x) g(x, \tau \mid x_0)]. \quad (82)$$

The explicit geometry dependence in Eq. 77 is now disguised by $g(x, \tau \mid x_0)$ and by the quasi-potential $\tilde{\phi}(x)$, and Eq. 82 has the "planar geometry form" for all values of the geometry parameter s. Some interesting consequences follow from this fact.

In terms of the propagator $g(x, \tau \mid x_0)$, free diffusion in any (radially symmetric) geometry is equivalent to diffusion in planar geometry in the presence of a repulsive logarithmic potential, e.g., $-\ln x$ for cylindrical and $-2 \ln x$ for spherical geometry. Conversely diffusion in a geometry s with a logarithmic potential, $\phi(x) = \alpha \ln x + \beta$, is equivalent to free diffusion in a space with geometry $s - \alpha$. Hence diffusion in an attractive potential, $\phi(x) = \ln x$, in cylindrical geometry is equivalent to free diffusion in planar geometry, whereas diffusion in a repulsive potential, $\phi(x) = -\ln x$, in cylindrical geometry is equivalent to free diffusion in spherical geometry.

In the case of the electric double layer, both parts of the quasi-potential are affected in the same direction by changes in geometry at constant surface charge density σ and constant $(b - a)$. Thus, as a increases toward infinity, both cylindrical ($s = 2$) and spherical ($s = 3$) geometry degenerate into planar ($s = 1$) geometry and $\tilde{\phi}(x)$ becomes more negative. As a consequence, $\tau_{PR}(x_0)$ decreases, while $\tau_{RP}(x_0)$ and $P_{PP}(\lambda \mid x_0)$ increase.

In this paper, we have considered the radial projection of the diffusion in three-dimensional spaces of various radially symmetric geometries. It is worth noting, however, that some of these results can be applied also to diffusion in two-dimensional spaces, i.e., to diffusion on surfaces of various geometries. Thus, the three-dimensional cylindrical diffusion problem is formally identical to the planar surface diffusion problem with a central potential. Similarly, the three-dimensional planar diffusion problem is formally identical to the cylindrical surface diffusion problem with a potential that depends only on the azimuthal angle. However, the spherical surface diffusion problem has no three-dimensional counterpart and must be treated in its own right. This has recently been done by Sano and Tachiya (36). We note that their result for the MAT can be obtained also by direct integration of the Smoluchowski equation.

LATERAL DIFFUSION AND SURFACE RE-ENCOUNTERS

In previous sections, we have considered only the radial propagator that describes diffusion normal to the bounding surfaces. Here we shall discuss also the lateral diffusion, i.e., diffusion parallel to the bounding surfaces. In particular, we ask for the root-mean-square lateral displacement of a counterion, initially located at the charged interface, during the mean time it takes to reach the radial coordinate $a + c$. Since the mean potential varies only in the radial direction, the lateral diffusion is free. Consequently, we have for planar geometry

$$\langle r^2 \rangle^{1/2} = [4D\tau_{RA}(0 \rightarrow c)]^{1/2}; \quad (83)$$

and for cylindrical geometry

$$\langle z^2 \rangle^{1/2} = [2D\tau_{RA}(a \rightarrow a + c)]^{1/2}, \quad (84)$$

where z is the axial displacement ($z = 0$ initially). An analogous relation for spherical geometry does not exist, because the spherical Laplacian does not contain an independent lateral part. However, the question of lateral diffusion is of lesser interest for spherical geometry

because of the absence of an infinite (or long compared with $b - a$) dimension under most conditions.

With the MAT formulae of Appendices B and C, Eqs. 83 and 84 yield

$$\frac{\langle r^2\rangle^{1/2}}{c} = \frac{b}{c}\frac{\sqrt{2}}{\gamma}\left\{\sin^2\left(\gamma\frac{c}{b}\right) + \tan\gamma\left[\gamma\frac{c}{b} - \sin\left(\gamma\frac{c}{b}\right)\cos\left(\gamma\frac{c}{b}\right)\right]\right\}^{1/2} \quad (85)$$

and

$$\frac{\langle z^2\rangle^{1/2}}{c} = \frac{b}{c}\frac{1}{\sqrt{2}\gamma}\left(\frac{(s^2+1)}{s^2}(C-1)\left[\left(\frac{a+c}{b}\right)^2 - \left(\frac{a}{b}\right)^2\right] + \frac{1}{s}\left[\frac{(s^2-3)}{(s^2+1)}C + 2\right]\left\{\left(\frac{a+c}{b}\right)^2 \cdot \sin\left[2s\ln\left(\frac{a+c}{b}\right)\right] - \left(\frac{a}{b}\right)^2\sin\left[2s\ln\left(\frac{a}{b}\right)\right]\right\} + \frac{1}{s^2}\left[\frac{(3s^2-1)}{(s^2+1)}C - (s^2-1)\right]\left\{\left(\frac{a+c}{b}\right)^2 \cdot \cos\left[2s\ln\left(\frac{a+c}{b}\right)\right] - \left(\frac{a}{b}\right)^2\cos\left[2s\ln\left(\frac{a}{b}\right)\right]\right\}\right)^{1/2}. \quad (86)$$

As written, Eq. 86 is valid for the strong coupling case as defined by Eq. C2*b*. In the free-diffusion limit, one gets

$$\frac{\langle r^2\rangle^{1/2}}{c} = \sqrt{2}; \quad (87)$$

$$\frac{\langle z^2\rangle^{1/2}}{c} = \left[\frac{1}{2} + \frac{a}{c} - \left(\frac{a}{c}\right)^2\ln\left(1 + \frac{c}{a}\right)\right]^{1/2}. \quad (88)$$

If $a \ll c$, then $\langle z^2\rangle^{1/2} = \langle r^2\rangle^{1/2}/2$, as expected. The rms lateral displacement before the counterion reaches the outer cell boundary is, for planar geometry,

$$\frac{\langle r^2\rangle^{1/2}}{b} = \left(\frac{2\tan\gamma}{\gamma}\right)^{1/2}; \quad (89)$$

and, for cylindrical geometry, in the limit $a \ll b$,

$$\frac{\langle z^2\rangle^{1/2}}{b} = \frac{[(s^2+5)C - (s^2+3)]^{1/2}}{\sqrt{2}\,(s^2+1)}. \quad (90)$$

From Figs. 16 and 17, in which we have plotted Eqs. 85 and 86 for typical strong coupling cases and for free diffusion, one can conclude that a strong electrostatic coupling may substantially enhance the rms lateral displacement of a counterion during its residence time in the cell. For very strong coupling, the counterion diffusion may thus be characterized as quasi–two-dimensional or quasi–one-dimensional in the planar and cylindrical cases, respectively.

Adam and Delbrück (9) discussed a two-stage process, whereby a ligand arrives at a surface-bound receptor by first diffusing to the surface, where it is adsorbed, and then proceeding to the receptor by surface diffusion. It was concluded that this reduction of the dimensionality of the diffusion space makes the two-stage process competitive, provided that the surface diffusion coefficient is not too small. While actual adsorption, e.g., by imbedding part of the diffusing molecule in the hydrocarbon interior of a lipid bilayer membrane, usually reduces the diffusion coefficient drastically, the counterion diffusion coefficient is not expected to vary significantly within the diffusion space. The double-layer interaction may thus be important in speeding up the binding of ionic ligands to receptors at charged interfaces.

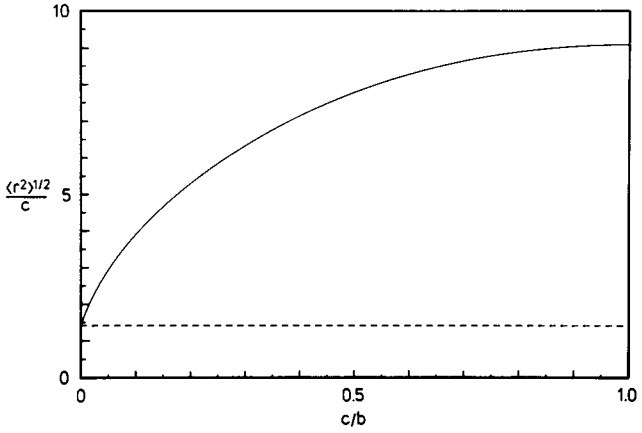

FIGURE 16 The rms lateral displacement, $\langle r^2\rangle^{1/2}$, of a counterion during the mean time required to diffuse a distance c out from the planar charged interface. The solid curve is an example of strong coupling (γ = 1.555245, C/λ = 100, ϕ_0 = −8.33), while the dashed line represents free diffusion (γ = 0).

The efficiency of a two-stage process for a nonadsorbed ligand is crucially dependent on the frequency with which it samples the receptor-bearing surface. It is therefore of

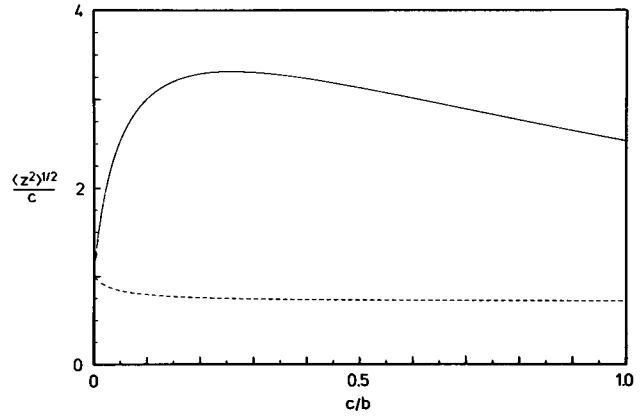

FIGURE 17 The rms axial displacement, $\langle z^2\rangle^{1/2}$, of a counterion during the mean time required to diffuse a distance c out from the cylindrical charged interface. The solid curve is an example of strong coupling (C = 5, λ = 0.02, ϕ_0 = −10.29), while the dashed curve represents free diffusion (C = 0, λ = 0.02).

interest to obtain an estimate of the mean total number, $N(\delta, c)$, of encounters with the interface, given that one has occurred, before the ligand reaches the radial coordinate $a + c$. In order to define a re-encounter within a continuous-space description of the ligand motion, we must introduce a distance δ: a collision with the surface is regarded as a re-encounter only if the ligand, since the last surface encounter, has sampled the region outside a distance δ from the surface.

Let $P_n(\delta, c)$ be the probability of having exactly n encounters before reaching the radial coordinate $a + c$. Then,

$$N(\delta, c) = \sum_{n=1}^{\infty} n P_n(\delta, c). \tag{91}$$

Since, after an encounter, the ligand arrives at radial coordinate $a + \delta$ with unit probability, we can express $P_n(\delta, c)$ in terms of the adsorption probability of Eq. 65 as

$$P_n(\delta, c) = [P_{AA}(a \mid a + \delta)]^{n-1} \cdot P_{AA}(a + c \mid a + \delta), \quad \delta < c. \tag{92}$$

Inserting this into Eq. 91, performing the geometric sum and using Eq. 65, we obtain

$$N(\delta, c) = \frac{J_0(a, a + c)}{J_0(a, a + \delta)}, \quad \delta < c. \tag{93}$$

Combination of Eqs. 50*a*, B2, and 93 yields for counterion diffusion in a planar double layer

$$N(\delta, c) = \frac{I_1(0, c)}{I_1(0, \delta)} = \frac{\gamma \frac{c}{b} + \sin\left(\gamma \frac{c}{b}\right) \cos\left[\gamma\left(2 - \frac{c}{b}\right)\right]}{\gamma \frac{\delta}{b} + \sin\left(\gamma \frac{\delta}{b}\right) \cos\left[\gamma\left(2 - \frac{\delta}{b}\right)\right]}, \quad \delta < c. \tag{94}$$

In the free-diffusion limit, this reduces to

$$N(\delta, c) = \frac{c}{\delta}, \quad \delta < c. \tag{95}$$

Eq. 94 is plotted in Fig. 18, from which we see that the electrostatic interaction may increase the number of surface encounters by several orders of magnitude. Because of the arbitrariness in the choice of δ, the exact numbers obtained for $N(\delta, c)$ are of limited significance. The trends, however, are suggestive.

As a final application, let us once more consider the process whereby a ligand becomes associated with a surface-bound receptor. We shall let α denote the fractional surface coverage of the receptors. The receptor patches, which can be of arbitrary shape, are characterized by an effective radius R. Ligands are absorbed on collision with receptor patches and reflected elsewhere.

We now ask for the conditional absorption probability,

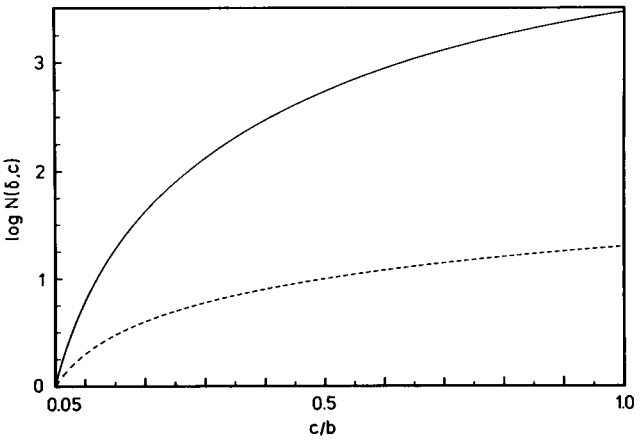

FIGURE 18 The conditional mean number of encounters, $N(\delta, c)$, of a counterion with the planar charged interface before it has receded a distance c out from the interface. Distinct encounters are separated by excursions that reach at least a distance $\delta = 0.05b$ out from the interface. The solid curve is an example of strong coupling ($\gamma = 1.555245$, $C/\lambda = 100$, $\phi_0 = -8.33$), while the dashed curve represents free diffusion ($\gamma = 0$).

P_{abs}, defined as the probability that a ligand that is known to have encountered the surface at least once will get absorbed by a receptor before it reaches the outer cell boundary. P_{abs} can be decomposed as

$$P_{abs}(\alpha) = \sum_{n=1}^{\infty} Q_n(\alpha), \tag{96}$$

where Q_n is the probability of a sequence of exactly $n - 1$ reflective surface encounters followed by an absorptive one, all prior to reaching the cell boundary. If successive encounters are independent and if each reflective encounter leaves the ligand at a distance δ from the surface, then

$$Q_n(\alpha) = \alpha[(1 - \alpha) P_{AA}(a \mid a + \delta)]^{n-1}. \tag{97}$$

If the distance between successive encounter points on the surface is less than the effective receptor radius R, then the encounters are clearly not independent. Given a reflective encounter, the probability of adsorption at the next encounter will then be $< \alpha$. As a rough condition for independence, we shall use $\delta = R$. This is plausible in the case of free diffusion (10), and it can be shown to be a sound choice also in the presence of a PB potential, provided that $R \ll b$. Setting $\delta = R$ and performing the geometric sum, we get

$$P_{abs}(\alpha) = \frac{\alpha}{1 - (1 - \alpha) P_{AA}(a \mid a + R)} = \left[1 + \frac{\frac{1}{\alpha} - 1}{N(R, b)}\right]^{-1}; \tag{98}$$

where the last equality follows from Eqs. 65*a* and 93.

We denote by $\alpha_{1/2}$ the receptor coverage required to

make $P_{abs} = 0.5$. According to Eq. 98

$$\alpha_{1/2} = \frac{1}{N(R, b) + 1}. \quad (99)$$

In the free-diffusion limit, Eqs. 95 and 99 yield

$$\alpha_{1/2} = \frac{1}{\frac{b}{R} + 1}. \quad (100)$$

Eq. 100 shows that, for a given catch ($P_{abs} = 0.5$), a smaller receptor coverage (fewer receptors) is needed if the total receptor area is finely dispersed (so that $R \ll b$). In other words, many small receptors catch more ligands than a few big ones (with the same total area). Moreover, it is seen that only a tiny fraction of the surface has to be covered by receptors to achieve $P_{abs} = 0.5$, provided that $R \ll b$. These points were made and discussed in detail by Berg and Purcell (10).

For free diffusion, the surface re-encounter phenomenon is a consequence of the random-walk nature of the ligand motion, according to which any imaginary plane (normal to the radial coordinate), once crossed, will be recrossed many times before the ligand has undergone an appreciable net displacement from the plane. In the presence of a potential, which, like the PB potential, forces the ligand toward the surface, the re-encounters should be even more numerous (see Fig. 18).

Fig. 19, which is based on Eqs. 94 and 99, shows how $\alpha_{1/2}$ varies with the receptor radius, R, for counterion diffusion in a planar double layer. We see that the electrostatic interaction can have a dramatic effect, lowering the necessary receptor surface coverage by several orders of magnitude. A numerical example may serve to further illustrate the effect. Consider a planar double layer with $b = 20$ nm consisting of monovalent counterions in water at 25°C outside a charged surface with one elementary charge per square nanometer. On the surface, circular receptors of radius 0.5 nm are arranged on a hexagonal lattice with a spacing of 50 nm. Although the receptors occupy only a fraction 3.6×10^{-4} of the surface, the catch of monovalent ligands is half of what it would be if the surface were completely covered by receptors. The biological and technological advantages of this phenomenon are obvious.

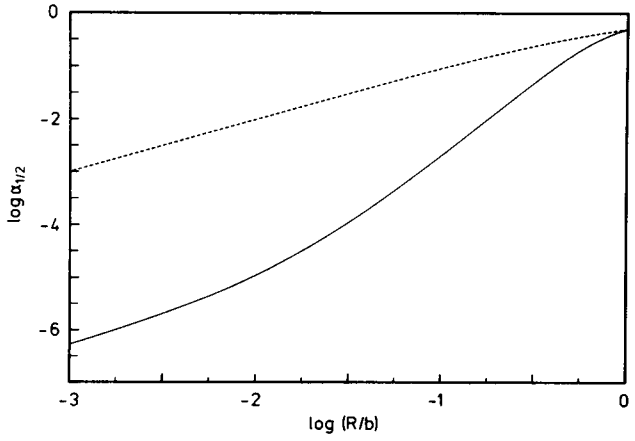

FIGURE 19 The receptor surface coverage $\alpha_{1/2}$, required to achieve half the maximum catch of ionic ligands at a planar charged surface vs. the effective receptor radius, R (in units of the fixed cell size, b). The solid curve is an example of strong coupling ($\gamma = 1.555245$, $C/\lambda = 100$, $\phi_0 = -8.33$), while the dashed curve represents free diffusion.

APPENDIX A

The Counterion Propagator in Planar Geometry

In this appendix, we solve the SPB equation for the counterion propagator in planar geometry (cf. Eq. 21):

$$\frac{\partial}{\partial \tau}\tilde{f}(\xi, \tau|\xi_0) = \frac{\partial}{\partial \xi}\left[\frac{\partial}{\partial \xi} - 2\tan\xi\right]\tilde{f}(\xi, \tau|\xi_0), \quad (A1)$$

subject to the initial condition (cf. Eq. 6)

$$\tilde{f}(\xi, 0|\xi_0) = \delta(\xi - \xi_0). \quad (A2)$$

The boundary conditions, corresponding to partial absorption at ξ_1 and ξ_2, are obtained from Eqs. 8a, 9, and 12 as

$$\cos\theta_1\,[\tilde{f}'(\xi_1, \tau|\xi_0) - 2\tan\xi_1\tilde{f}(\xi_1, \tau|\xi_0)] - \sin\theta_1\tilde{f}(\xi_1, \tau|\xi_0) = 0; \quad (A3a)$$

$$\cos\theta_2\,[\tilde{f}'(\xi_2, \tau|\xi_0) - 2\tan\xi_2\tilde{f}(\xi_2, \tau|\xi_0)] + \sin\theta_2\tilde{f}(\xi_2, \tau|\xi_0) = 0; \quad (A3b)$$

where we have replaced the absorption coefficients of Eq. 9 by

$$\theta_i \equiv \arctan\left(\frac{b\kappa_i}{\gamma D}\right). \quad (A4)$$

A perfectly reflecting boundary corresponds to $\theta_i = 0$ and a perfectly absorbing one to $\theta_i = \pi/2$.

We attempt a solution of the form

$$\tilde{f}(\xi, \tau|\xi_0) = \Theta(\xi)\,\Upsilon(\tau). \quad (A5)$$

Substitution into Eq. A1 yields

$$\frac{\Upsilon'(\tau)}{\Upsilon(\tau)} = \frac{\Theta''(\xi)}{\Theta(\xi)} - 2\tan\xi\frac{\Theta'(\xi)}{\Theta(\xi)} - 2\sec^2\xi = -(\lambda^2 - 1), \quad (A6)$$

where we have denoted the separation constant by $-(\lambda^2 - 1)$. The time-dependent part of the solution is obtained immediately from Eq. A6 as

$$\Upsilon(\tau) = \exp[-(\lambda^2 - 1)\tau]. \quad (A7)$$

The spatial part is the solution to the second-order ordinary differential equation

$$\Theta''(\xi) - 2\tan\xi\,\Theta'(\xi) + [\lambda^2 - 1 - 2\sec^2\xi]\,\Theta(\xi) = 0. \quad (A8)$$

By introducing the new dependent variable

$$y(\xi) \equiv \cos\xi\,\Theta(\xi), \quad (A9)$$

we can transform Eq. A8 into normal form, lacking the first derivative,

$$y''(\xi) + [\lambda^2 - 2\sec^2\xi]\, y(\xi) = 0. \tag{A10}$$

As can easily be verified, the general solution to Eq. A10 is

$$y(\xi) = \alpha[\tan\xi\cos\lambda\xi - \lambda\sin\lambda\xi] + \beta[\tan\xi\sin\lambda\xi + \lambda\cos\lambda\xi], \tag{A11}$$

where α and β are constants to be determined from the initial and boundary conditions.

The boundary conditions on $y(\xi)$ follow from Eqs. A3, A5, and A9:

$$\cos\theta_1[y'(\xi_1) - \tan\xi_1\, y(\xi_1)] - \sin\theta_1\, y(\xi_1) = 0; \tag{A12a}$$

$$\cos\theta_2[y'(\xi_2) - \tan\xi_2\, y(\xi_2)] + \sin\theta_2\, y(\xi_2) = 0; \tag{A12b}$$

Inserting $y(\xi)$ and $y'(\xi)$ from Eq. A11, we find that Eq. A12 will only have the physically uninteresting solution $\alpha = \beta = 0$, i.e., $y(\xi) = 0$, for arbitrary values of λ. However, if λ takes on special values, the so-called eigenvalues λ_n ($n = 0, 1, 2, \ldots$), then α and β may be nonzero. These eigenvalues are obtained by requiring the determinant of the coefficients of α and β in Eq. A12 to vanish. This results in the eigenvalue equation

$$\begin{aligned}\cot[\lambda_n(\xi_2 - \xi_1)]\,[(\lambda_n^2 - 1)\sin(\theta_1 + \theta_2)\cos\xi_1\cos\xi_2 \\ - \sin\theta_1\sin\theta_2\sin(\xi_2 - \xi_1)] = (\lambda_n^2 - 1) \\ \cdot [\lambda_n\cos\theta_1\cos\theta_2\cos\xi_1\cos\xi_2 \\ - \lambda_n^{-1}\cos(\theta_1 + \xi_1)\cos(\theta_2 - \xi_2)] \\ - \lambda_n\sin\theta_1\sin\theta_2\cos(\xi_2 - \xi_1); \\ n = 0, 1, 2, \ldots.\end{aligned} \tag{A13}$$

According to Eq. A11, we can write the eigenfunctions of Eq. A10 as

$$y_n(\xi) = \alpha_n u_n(\xi) + \beta_n v_n(\xi), \tag{A14}$$

where

$$u_n(\xi) \equiv \tan\xi\cos\lambda_n\xi - \lambda_n\sin\lambda_n\xi; \tag{A15a}$$

$$v_n(\xi) \equiv \tan\xi\sin\lambda_n\xi + \lambda_n\cos\lambda_n\xi. \tag{A15b}$$

The eigenfunctions $y_n(\xi)$ are easily shown to be orthogonal on the interval $[\xi_1, \xi_2]$:

$$\int_{\xi_1}^{\xi_2} d\xi\, y_m(\xi)\, y_n(\xi) = \delta_{mn} N_n, \tag{A16}$$

with the normalization constant given by

$$\begin{aligned}N_n = \frac{1}{2}(\alpha_n^2 + \beta_n^2)(\lambda_n^2 - 1)(\xi_2 - \xi_1) \\ + \tan\xi_2[\alpha_n\cos\lambda_n\xi_2 + \beta_n\sin\lambda_n\xi_2]^2 \\ - \tan\xi_1[\alpha_n\cos\lambda_n\xi_1 + \beta_n\sin\lambda_n\xi_1]^2 \\ - \frac{1}{2}(\lambda_n + \lambda_n^{-1})\sin[\lambda_n(\xi_2 - \xi_1)] \\ \cdot \{(\alpha_n^2 - \beta_n^2)\cos[\lambda_n(\xi_1 + \xi_2)] \\ + 2\alpha_n\beta_n\sin[\lambda_n(\xi_1 + \xi_2)]\}.\end{aligned} \tag{A17}$$

From Eqs. A5, A7, and A9, we have

$$\tilde{f}(\xi, \tau\,|\,\xi_0) = \sec\xi\sum_{n=0}^{\infty} g_n(\xi_0) y_n(\xi)\exp[-(\lambda_n^2 - 1)\tau]. \tag{A18}$$

Setting $\tau = 0$ and using Eq. A2,

$$\delta(\xi - \xi_0) = \sec\xi\sum_{n=0}^{\infty} g_n(\xi_0)\, y_n(\xi). \tag{A19}$$

Multiplying by $\cos\xi\, y_m(\xi)$ and integrating over ξ, using Eq. A16, we get

$$g_n(\xi_0) = \kappa N_n^{-1}\cos\xi_0\, y_n(\xi_0), \tag{A20}$$

which is inserted into Eq. A18 to give

$$\tilde{f}(\xi, \tau\,|\,\xi_0) = \frac{\cos\xi_0}{\cos\xi}\sum_{n=0}^{\infty} \cdot\left[\frac{y_n(\xi_0)\, y_n(\xi)}{N_n}\right]\exp[-(\lambda_n^2 - 1)\tau]. \tag{A21}$$

Together with Eqs. A13–A17, this represents the general solution to our problem. As can be seen from Eqs. A14 and A17, the term within square brackets in Eq. A21 depends only on the ratio α_n/β_n (or β_n/α_n). This ratio is obtained from Eq. A12*a* or A12*b* as a function of θ_1, ξ_1, and λ_n or θ_2, ξ_2, and λ_n. As noted in the main text, in the case that both boundaries are perfectly reflecting ($\theta_1 = \theta_2 = 0$), one must add the equilibrium distribution $f(\xi)$ from Eq. 23 to the right-hand side of Eq. A21.

The probability, $Q(\tau)$, that a given counterion has not yet been absorbed at one of the boundaries at time τ is given by Eq. 25, which can be combined with Eqs. 23, A14, A15, and A21 and then integrated to give

$$\begin{aligned}Q(\tau) = [\tan\xi_2 - \tan\xi_1]^{-1} \\ \cdot \sum_{n=0}^{\infty} N_n^{-1}\{\sec\xi_2[\alpha_n\cos\lambda_n\xi_2 + \beta_n\sin\lambda_n\xi_2] \\ - \sec\xi_1[\alpha_n\cos\lambda_n\xi_1 + \beta_n\sin\lambda_n\xi_1]\}^2 \\ \cdot \exp[-(\lambda_n^2 - 1)\tau].\end{aligned} \tag{A22}$$

The mean time to adsorption, τ_{abs}, is given by Eq. 26, which can be combined with Eq. A22 and then integrated to give

$$\begin{aligned}\tau_{abs} = [\tan\xi_2 - \tan\xi_1]^{-1} \\ \cdot \sum_{n=0}^{\infty}(\lambda_n^2 - 1)^{-1} N_n^{-1} \\ \cdot \{\sec\xi_2[\alpha_n\cos\lambda_n\xi_2 + \beta_n\sin\lambda_n\xi_2] \\ - \sec\xi_1[\alpha_n\cos\lambda_n\xi_1 + \beta_n\sin\lambda_n\xi_1]\}^2.\end{aligned} \tag{A23}$$

In the remainder of this appendix, we present some special cases of the general solution. In these special cases, the boundaries of the counterion diffusion space are taken to coincide with the charged interface and the midplane ($c_1 = -b$ and $c_2 = 0$ in Fig. 2). The boundary conditions considered are perfect reflection and perfect absorption. To facilitate comparison with the cylindrical and spherical cases, we shift the origin of coordinates to the charged interface. Moreover, we let x denote the distance from the charged interface, measured in units of the cell "radius" b. The charged interface is thus located at $x = 0$ and the midplane (outer cell boundary) at $x = 1$. Furthermore, we transform back from τ to t according to Eq. 19, so that time is now measured in seconds. To conform with the notation used elsewhere in this paper, we shall indicate the nature of the boundaries by subscripts on the mean absorption time.

Case I: Reflection at the Charged Interface and Absorption at the Midplane.

$$\lambda_n = \frac{(2n+1)\pi}{2\gamma}; \quad n = 0, 1, 2, \ldots; \tag{A24}$$

$$y_n(x) = (-1)^{n+1}\alpha_n\left\{\tan[\gamma(1-x)]\sin\left[(2n+1)\frac{\pi}{2}x\right] - \frac{(2n+1)\pi}{2\gamma}\cos\left[(2n+1)\frac{\pi}{2}x\right]\right\}; \tag{A25}$$

$$N_n = \frac{\alpha_n^2}{2\gamma}\left\{\left[(2n+1)\frac{\pi}{2}\right]^2 - \gamma_2\right\}; \tag{A26}$$

$$Q(t) = 2\gamma\cot\gamma\sum_{n=0}^{\infty}\left\{\left[(2n+1)\frac{\pi}{2}\right]^2 - \gamma^2\right\}^{-1} \exp\left[-\left\{\left[(2n+1)\frac{\pi}{2}\right]^2 - \gamma^2\right\}\frac{Dt}{b^2}\right]; \tag{A27}$$

$$\tau_{RA} = \frac{b^2}{2D\gamma}\left[\tan\gamma + \cot\gamma - \frac{1}{\gamma}\right]. \tag{A28}$$

Case II: Absorption at the Charged Interface and Reflection at the Midplane. To obtain the eigenvalues λ_n, we must solve the transcendental equation

$$\lambda_n\cot\lambda_n\gamma + \tan\gamma = 0; \quad n = 0, 1, 2, \ldots. \tag{A29}$$

The solutions to Eq. A29 are given by the intersections of the curves $\cot\lambda_n\gamma$ with the curve $-\gamma\tan\gamma/\lambda_n\gamma$, as shown in Fig. 20. It is seen that the eigenvalues are confined to the ranges

$$\frac{\left(n+\frac{1}{2}\right)\pi}{\gamma} < \lambda_n < \frac{(n+1)\pi}{\gamma}; \quad n = 0, 1, 2, \ldots. \tag{A30}$$

The remaining results for this case are

$$y_n(x) = \beta_n\{\tan[\gamma(1-x)]\sin[\lambda_n\gamma(1-x)] + \lambda_n\cos[\lambda_n\gamma(1-x)]\}; \tag{A31}$$

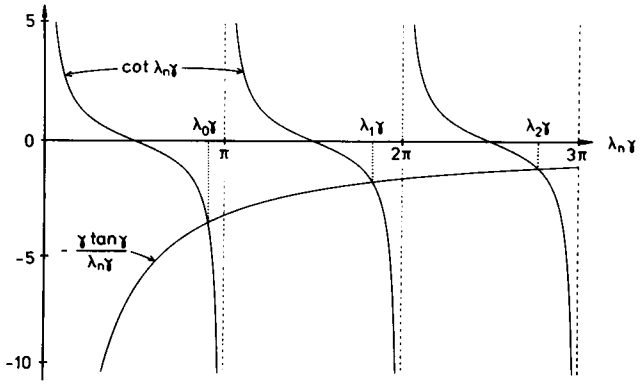

FIGURE 20 Graphical solution of the eigenvalue Eq. A29 (with $\gamma\tan\gamma = 10$).

$$N_n = \frac{\beta_n^2}{2}(\lambda_n^2 - 1)[\gamma + \cot\gamma\cos^2\lambda_n\gamma]; \tag{A32}$$

$$Q(t) = 2\csc 2\gamma\sum_{n=0}^{\infty}\beta_n^2 N_n^{-1}\sin^2\lambda_n\gamma \cdot \exp\left\{-[(\lambda_n\gamma)^2 - \gamma^2]\frac{Dt}{b^2}\right\}; \tag{A33}$$

$$\tau_{AR} = \frac{b^2}{2D\gamma}\left[\cot\gamma - \frac{\cos^2\gamma}{\gamma}\right]. \tag{A34}$$

From Fig. 20 it is clear that in the strong coupling regime, where $\gamma \approx \pi/2$, λ_n approaches $(n+1)\pi/\gamma$. However, in contrast to case I, this does not cause $Q(t)$ to be dominated by a single (slowly decaying) exponential. The reason is the obvious fact that the electrostatic interaction only retards counterion diffusion away from the charged interface.

Case III: Absorption at the Charged Interface and at the Midplane.

$$\lambda_n\tan\lambda_n\gamma - \tan\gamma = 0; \quad n = 0, 1, 2, \ldots; \tag{A35}$$

$$y_n(x) = -\alpha_n\{\tan[\gamma(1-x)]\cos[\lambda_n\gamma(1-x)] - \lambda_n\sin[\lambda_n\gamma(1-x)]\}; \tag{A36}$$

$$N_n = \frac{\alpha_n^2}{2}(\lambda_n^2 - 1)[\gamma + \cot\gamma\sin^2\lambda_n\gamma]; \tag{A37}$$

$$Q(t) = \cot\gamma\sum_{n=0}^{\infty}\alpha_n^2 N_n^{-1}[1 - \sec\gamma\cos\lambda_n\gamma]^2 \cdot \exp\left\{-[(\lambda_n\gamma)^2 - \gamma^2]\frac{Dt}{b^2}\right\}; \tag{A38}$$

$$\tau_{AA} = \frac{b^2}{2D\gamma}\left\{\cot\gamma - \left[\frac{2\cos^2\gamma + \sin 2\gamma/\gamma}{2\gamma + \sin 2\gamma}\right]\right\}. \tag{A39}$$

Case IV: Reflection at the Charged Interface and at the Midplane.

$$\lambda_n = \frac{(n+1)\pi}{\gamma}; \quad n = 0, 1, 2, \ldots; \tag{A40}$$

$$y_n(x) = (-1)^n\beta_n\left\{\tan[\gamma(1-x)]\sin[(n+1)\pi x] - \frac{(n+1)\pi}{\gamma}\cos[(n+1)\pi x]\right\}; \tag{A41}$$

$$N_n = \frac{\beta_n^2}{2\gamma}\{[(n+1)\pi]^2 - \gamma^2\}. \tag{A42}$$

The propagator evolves toward the equilibrium distribution

$$f(x) = \frac{\gamma}{b}\cot\gamma\sec^2[\gamma(1-x)], \tag{A43}$$

and, since no absorption takes place, $Q(t) = 1$ and $\tau_{RR} = \infty$.

APPENDIX B

MATs and Absorption Probabilities for Planar Geometry

With the charged interface at $x = 0$ and the other cell boundary at $x = b$, the reduced PB potential takes the form (12, 14)

$$\phi(x) = 2 \ln \cos \gamma(1 - x), \tag{B1}$$

where $x \equiv r/b$ and $\lambda \equiv \kappa b$, the latter quantity being obtained from Eq. 15. Substitution into Eq. 49 yields

$$I_1(x_1, x_2) = \int_{x_1}^{x_2} dx \cos^2 \gamma(1 - x) = \frac{1}{2\gamma} \cdot [\gamma(x_2 - x_1) + \sin \gamma(x_2 - x_1) \cos \gamma(2 - x_1 - x_2)]. \tag{B2}$$

Using Eqs. 17, B1, and B2, we find that Eqs. 53 and 55 (with $\lambda = 0$) yield

$$\tau_{RP}(x_0) = \frac{b \tan \gamma}{\kappa_b \gamma} + \frac{b^2}{2D\gamma^2}\left\{(1 - x_0)\gamma \tan \gamma + \frac{1}{2} \sin 2\gamma(1 - x_0)[\tan \gamma - \tan \gamma(1 - x_0)]\right\}; \tag{B3}$$

$$\tau_{RP}(0) = \left(\frac{b}{\kappa_b} + \frac{b^2}{2D}\right)\frac{\tan \gamma}{\gamma}; \tag{B4}$$

$$\tau_{PR}(x_0) = \frac{b \sin 2\gamma}{2\kappa_a \gamma} + \frac{b^2}{2D\gamma^2}[\cos^2 \gamma(1 - x_0) - \cos^2 \gamma]; \tag{B5}$$

$$\tau_{PR}(1) = \frac{b \sin 2\gamma}{2\kappa_a \gamma} + \frac{b^2 \sin^2 \gamma}{2D\gamma^2}; \tag{B6}$$

$$\tau_{AA}(x_0) = \frac{b^2}{2D\gamma^2}\left\{\left[\frac{2\gamma(1 - x_0) + \sin 2\gamma(1 - x_0)}{2\gamma + \sin 2\gamma}\right] \cdot \sin^2 \gamma - \sin^2 \gamma(1 - x_0)\right\}; \tag{B7}$$

$$\tau_{RP} = \frac{b \tan \gamma}{\kappa_b \gamma} + \frac{b^2}{2D\gamma}\left[\tan \gamma + \cot \gamma - \frac{1}{\gamma}\right]; \tag{B8}$$

$$\tau_{PR} = \frac{b \sin 2\gamma}{2\kappa_a \gamma} + \frac{b^2}{2D\gamma}\left[\cot \gamma - \frac{\cos^2 \gamma}{\gamma}\right]; \tag{B9}$$

$$\tau_{AA} = \frac{b^2}{2D\gamma}\left[\cot \gamma - \left(\frac{2 \cos^2 \gamma + \sin 2\gamma/\gamma}{2\gamma + \sin 2\gamma}\right)\right]. \tag{B10}$$

Eqs. B3 and B4, in the special case $\kappa_b = \infty$, have appeared previously in the literature (26).

It is straightforward to derive MAT formulae also for diffusion in the entire interlamellar space, with charged interfaces at $x = \pm 1$. As an example, we consider the mean time taken for a counterion to reach the coordinate x for the first time, starting at the charged interface $x = -1$. According to Eq. 39*a*,

$$\tau_{RA}(-1 \to x) = \bar{J}_1(-1, x), \tag{B11}$$

so that

$$\tau_{RA}(-1 \to x) = \frac{b^2}{2D\gamma^2}\{\tan \gamma [\gamma(1 + x) + \sin \gamma(1 + x) \cos \gamma(1 - x)] + \cos^2 \gamma - \cos^2 \gamma x\}, \tag{B12}$$

with the special case

$$\tau_{RA}(-1 \to 1) = \frac{b^2}{D}\left(\frac{\tan \gamma}{\gamma} + \frac{\sin^2 \gamma}{\gamma^2}\right). \tag{B13}$$

Using Eqs. 17, 72, B1, and B2, we obtain the absorption probabilities

$$P_{AA}(0 \mid x_0) = \frac{2\gamma(1 - x_0) + \sin^2 \gamma(1 - x_0)}{2\gamma + \sin 2\gamma}; \tag{B14}$$

$$P_{AA}(0) = \frac{2\gamma}{2\gamma + \sin 2\gamma}. \tag{B15}$$

For diffusion in the entire interlamellar space, with charged interfaces at $x = \pm 1$, we get

$$P_{AA}(-1 \mid x_0) = \frac{1}{2}\left[1 - \left(\frac{2\gamma x_0 + \sin 2\gamma x_0}{2\gamma + \sin 2\gamma}\right)\right]. \tag{B16}$$

APPENDIX C

MATs and Absorption Probabilities for Cylindrical Geometry

Apart from the coupling parameter C and the cell size parameter λ, it is convenient to introduce also the (positive) quantity

$$\eta \equiv -\ln \lambda. \tag{C1}$$

The equations take on slightly different forms depending on whether one has the weak coupling case, with

$$C < \eta(1 + \eta)^{-1} \quad \text{and} \quad \gamma < 1 \tag{C2a}$$

or the strong coupling case, with

$$C > \eta(1 + \eta)^{-1} \quad \text{and} \quad \gamma > 1 \tag{C2b}$$

We shall give only the strong coupling results. The corresponding weak coupling formulae are obtained simply by replacing the parameter s (not to be confused with the geometry parameter) by $i\,s$ everywhere.

In the strong coupling case, we define the parameter s through

$$\gamma \equiv (s^2 + 1)^{1/2}. \tag{C3}$$

It is obtained by solving the transcendental equation

$$(s^2 + 1)[s \cot (s\eta) + 1]^{-1} = C. \tag{C4}$$

The reduced PB potential is given by (12, 13)

$$\phi(x) = 2 \ln\left\{x\left[\cos (s \ln x) - \frac{1}{s} \sin (s \ln x)\right]\right\}, \tag{C5}$$

where $x \equiv r/b$. Substitution into Eq. 49 yields

$$I_2(x_1, x_2) = \frac{x_2^2}{4}\left[\frac{(s^2 + 1)}{s^2} + \frac{(s^2 - 3)}{s(s^2 + 1)} \sin (2s \ln x_2) + \frac{(3s^2 - 1)}{s^2(s^2 + 1)} \cos (2s \ln x_2)\right] - \frac{x_1^2}{4} \cdot \left[\frac{(s^2 + 1)}{s^2} + \frac{(s^2 - 3)}{s(s^2 + 1)} \sin (2s \ln x_1) + \frac{(3s^2 - 1)}{s^2(s^2 + 1)} \cos (2s \ln x_1)\right]. \tag{C6}$$

Using Eqs. C3–C6, we find that Eqs. 53 and 55 yield

$$\tau_{RP}(x_0) = \frac{b^2 C}{\kappa_b (s^2+1)} + \frac{b^2}{4D(s^2+1)}\left(\left[\frac{(s^2+5)}{(s^2+1)}C - 2\right] - \frac{x_0^2}{s^2}\left\{(C-1)(s^2+1) + \left[\frac{(s^2-3)}{(s^2+1)}C + 2\right] \cdot s \sin(2s \ln x_0) + \left[\frac{(3s^2-1)}{(s^2+1)}C - (s^2-1)\right] \cdot \cos(2s \ln x_0)\right\}\right); \quad \text{(C7)}$$

$$\tau_{PR}(x_0) = \frac{a^2(s^2+1)\sin^2(s\eta)}{\kappa_a s^2 C} + \frac{b^2}{2D(s^2+1)}\left\{x_0^2\left[\cos(s \ln x_0) - \frac{1}{s}\sin(s \ln x_0)\right]^2 - \lambda^2\left[\cos(s\eta) + \frac{1}{s}\sin(s\eta)\right]^2\right\}; \quad \text{(C8)}$$

$$\tau_{RP} = \frac{b^2 C}{\kappa_b (s^2+1)} + \frac{b^2}{D}\left[\frac{1}{4C} - \frac{1}{(s^2+1)} + \frac{(s^2+5)C}{4(s^2+1)^2}\right] + \lambda^2\left\{\frac{(s^2+1)\sin^2(s\eta)}{2s^2 C^2} - \frac{1}{4C} - \frac{C}{4s^2(s^2+1)^2}[(s^2+1)^2 - s(s^2-3)\sin(2s\eta) + (3s^2-1)\cos(2s\eta)]\right\}; \quad \text{(C9)}$$

$$\tau_{PR} = \frac{a^2(s^2+1)\sin^2(s\eta)}{\kappa_a s^2 C} + \frac{b^2}{4DC}\left\{1 - \lambda^2\left[1 + \frac{2(s^2+1)\sin^2(s\eta)}{s^2 C}\right]\right\}. \quad \text{(C10)}$$

Eq. C9 (with $\kappa_b = \infty$) has recently been used in connection with the interpretation of counterion spin relaxation in polyelectrolyte solutions (37).

Combining Eqs. 72a and C6, we obtain the absorption probability

$$P_{AA}(\lambda | x_0) = \frac{\begin{array}{c} s^2(s^2+5) - x_0^2[(s^2+1)^2 \\ + s(s^2-3)\sin(2s \ln x_0) \\ + (3s^2-1)\cos(2s \ln x_0)] \end{array}}{\begin{array}{c} s^2(s^2+5) - \lambda^2[(s^2+1)^2 \\ - s(s^2-3)\sin(2s\eta) \\ + (3s^2-1)\cos(2s\eta)] \end{array}}. \quad \text{(C11)}$$

APPENDIX D

Absorption Probabilities by Direct Integration of the Smoluchowski Equation

In this appendix, we show how the general Eq. 65 for the absorption probabilities can be derived by the direct integration method used by Deutch (29) in the case of the MAT. We begin by noting that the probability of absorption at a particular boundary is just the accumulated flux across that boundary, i.e.,

$$P_{PP}(a | r_0) = -\int_0^\infty dt\, a^{s-1} j(a, t | r_0). \quad \text{(D1)}$$

Direct integration of the continuity Eq. 7 from a to r yields

$$r^{s-1} j(r, t | r_0) - a^{s-1} j(a, t | r_0) = -\int_a^r dr'\, r'^{s-1} \frac{\partial}{\partial t} f(r', t | r_0). \quad \text{(D2)}$$

Setting $r = b$, we obtain a relation between the boundary fluxes

$$b^{s-1} j(b, t | r_0) - a^{s-1} j(a, t | r_0) = -\int_a^b dr' r'^{s-1} \frac{\partial}{\partial t} f(r', t | r_0). \quad \text{(D3)}$$

We now multiply Eq. D2 by $r^{1-s} e^{\phi(r)}/D(r)$ and integrate from a to b:

$$-\int_a^b dr \frac{e^{\phi(r)}}{D(r)} j(r, t | r_0) + a^{s-1} j(a, t | r_0) \int_a^b dr\, r^{1-s} \frac{e^{\phi(r)}}{D(r)} = \int_a^b dr\, r^{1-s} \frac{e^{\phi(r)}}{D(r)} \int_a^r dr'\, r'^{s-1} \frac{\partial}{\partial t} f(r', t | r_0). \quad \text{(D4)}$$

Using, in turn, the flux density expression of Eq. 8b, the boundary conditions of Eq. 9, and the flux relation Eq. D3, we can transform the first integral in Eq. D4 as follows:

$$\begin{aligned} -\int_a^b dr \frac{e^{\phi(r)}}{D(r)} j(r, t | r_0) &= e^{\phi(b)} f(b, t | r_0) - e^{\phi(a)} f(a, t | r_0) \\ &= \frac{1}{\kappa_b} e^{\phi(b)} b^{s-1} j(b, t | r_0) + \frac{1}{\kappa_a} e^{\phi(a)} a^{s-1} j(a, t | r_0) \\ &= \left[\frac{1}{\kappa_a} e^{\phi(a)} + \frac{1}{\kappa_b} e^{\phi(b)}\right] a^{s-1} j(a, t | r_0) \\ &\quad - \frac{1}{\kappa_b} e^{\phi(b)} \int_a^b dr'\, r'^{s-1} \frac{\partial}{\partial t} f(r', t | r_0). \end{aligned} \quad \text{(D5)}$$

Inserting this expression into Eq. D4, we get

$$a^{s-1} j(a, t | r_0) = \frac{\begin{array}{c} \frac{1}{\kappa_b} e^{\phi(b)} \int_a^b dr'\, r'^{s-1} \frac{\partial}{\partial t} f(r', t | r_0) \\ + \int_a^b dr\, r^{1-s} \frac{e^{\phi(r)}}{D(r)} \int_a^r dr'\, r'^{s-1} \frac{\partial}{\partial t} f(r', t | r_0) \end{array}}{\frac{1}{\kappa_a} e^{\phi(a)} + \frac{1}{\kappa_b} e^{\phi(b)} + \int_a^b dr\, r^{1-s} \frac{e^{\phi(r)}}{D(r)}}. \quad \text{(D6)}$$

Finally, we integrate Eq. D6 over time, using the definition Eq. D1, the initial condition Eq. 6, and $f(r, \infty | r_0) = 0$:

$$P_{PP}(a | r_0) = \frac{\frac{1}{\kappa_b} e^{\phi(b)} + \int_{r_0}^b dr\, r^{1-s} \frac{e^{\phi(r)}}{D(r)}}{\frac{1}{\kappa_a} e^{\phi(a)} + \frac{1}{\kappa_b} e^{\phi(b)} + \int_a^b dr\, r^{1-s} \frac{e^{\phi(r)}}{D(r)}}. \quad \text{(D7)}$$

If we multiply the numerator and denominator by $\kappa_a \kappa_b f(a) f(b) \int_a^b dr\, r^{s-1} e^{-\phi(r)}$ and then use the definitions Eqs. 10 and 37, we arrive at the desired expression, Eq. 65a.

Received for publication 16 January 1984 and in final form 16 April 1984.

REFERENCES

1. Gouy, G. 1910. Sur la constitution de la charge electrique a la surface d'un electrolyte. *J. Phys.* 9:457–468.
2. Chapman, D. L. 1913. A contribution to the theory of electrocapillarity. *Philos. Mag.* 25:475–481.
3. Debye, P. 1942. Reaction rates in ionic solutions. *Trans. Electrochem. Soc.* 82:265–272.
4. Hammes, G. G., and R. A. Alberty. 1959. The influence of the net protein charge on the rate of formation of enzyme-substrate complexes. *J. Phys. Chem.* 63:274–279.
5. Richter, P. H., and M. Eigen. 1974. Diffusion controlled reaction rates in spheroidal geometry. Application to repressor-operator association and membrane bound enzymes. *Biophys. Chem.* 2:255–263.
6. Wiegel, F. W. 1983. Diffusion and the physics of chemoreception. *Phys. Rep.* 95:283–319.
7. von Smoluchowski, M. 1915. Über Brownsche Molekularbewegung unter Einwirkung äusserer Kräfte und deren Zusammenhang mit der verallgemeinerten Diffusionsgleichung. *Ann. Physik. (Berl.).* 48:1103–1112.
8. Verwey, E. J. W., and J. Th. G. Overbeek. 1948. Theory of the Stability of Lyophobic Colloids. Elsevier/North-Holland Biomedical Press, Amsterdam. 66–133.
9. Adam, G., and M. Delbrück. 1968. Reduction of dimensionality in biological diffusion processes. *In* Structural Chemistry and Molecular Biology. A. Rich and N. Davidson, editors. W.H. Freeman & Co., San Francisco, CA. 198–215.
10. Berg, H. C., and E. M. Purcell. 1977. Physics of chemoreception. *Biophys. J.* 20:193–219.
11. Noyes, R. M. 1954. A treatment of chemical kinetics with special applicability to diffusion controlled reactions. *J. Chem. Phys.* 22:1349–1359.
12. Lemke, H. 1913. Über die Differentialgleichungen, welche den Gleichgewichtszustand eines gasförmigen Himmelskörpers bestimmen, dessen Teile gegeneinander nach dem Newtonschen Gesetze gravitieren. *J. Math. (Berl.).* 142:118–145.
13. Fuoss, R. M., A. Katchalsky, and S. Lifson. 1951. The potential of an infinite rod-like molecule and the distribution of counterions. *Proc. Natl. Acad. Sci. USA.* 37:579–589.
14. Ohnishi, T., N. Imai, and F. Oosawa. 1960. Interaction between rod-like polyelectrolytes. *J. Phys. Soc. Jpn.* 15:896–905.
15. Fehder, P. L., C. A. Emeis, and R. P. Futrelle. 1971. Microscopic mechanism for self-diffusion and relative diffusion in simple liquids. *J. Chem. Phys.* 54:4921–4934.
16. Northrup, S. H., and J. T. Hynes. 1979. Short range caging effects for reactions in solution. I. Reaction rate constants and short range caging picture. *J. Chem. Phys.* 71:871–883.
17. Monchick, L. 1956. Note on the theory of diffusion controlled reactions: application to photodissociation in solution. *J. Chem. Phys.* 24:381–385.
18. Tachiya, M. 1979. Recombination of geminate species in the presence of a scavenger. *J. Chem. Phys.* 70:238–241.
19. Morse, P. M., and H. Feshbach. 1953. Methods of Theoretical Physics. McGraw-Hill, New York. 1584–1757.
20. Wheelon, A. D. 1968. Tables of Summable Series and Integrals Involving Bessel Functions. Holden-Day, San Francisco, CA. 125.
21. Weiss, G. H. 1967. First passage time problems in chemical physics. *Adv. Chem. Phys.* 13:1–18.
22. Schrödinger, E. 1915. Zur Theorie der Fall- und Steigversuche an Teilchen mit Brownscher Bewegung. *Phys. Z.* 16:289–295.
23. von Smoluchowski, M. 1915. Notiz über die Berechnung der Brownschen Molekularbewegung bei der Ehrenhaft-Millikanschen Versuchsanordning. *Phys. Z.* 16:318–321.
24. Pontrjagin, L., A. Andronoff, and A. Witt. 1934. Statistische Auffassung dynamischer Systeme. *Phys. Z. Sowjet.* 6:1–24.

24a. Pontrjagin, L., A. Andronoff, and A. Witt. 1933. *Zh. Eksp. Teor. Fiz.* 3:172.

25. Klein, G. 1952. Mean first-passage times of Brownian motion and related problems. *Proc. R. Soc. Lond. A.* 211:431–443.
26. Lifson, S., and J. L. Jackson. 1962. On the self-diffusion of ions in a polyelectrolyte solution. *J. Chem. Phys.* 36:2410–2414.
27. Goel, N. S., and N. Richter-Dyn. 1974. Stochastic Models in Biology. Academic Press, Inc., New York. 261.
28. Szabo, A., K. Schulten, and Z. Schulten. 1980. First passage time approach to diffusion controlled reactions. *J. Chem. Phys.* 72:4350–4357.
29. Deutch, J. M. 1980. A simple method for determining the mean passage time for diffusion controlled processes. *J. Chem. Phys.* 73:4700–4701.
30. Onsager, L. 1938. Initial recombination of ions. *Phys. Rev.* 54:554–557.
31. Tachiya, M. 1978. General method for calculating the escape probability in diffusion-controlled reactions. *J. Chem. Phys.* 69:2375–2376.
32. Sano, H., and M. Tachiya. 1979. Partially diffusion-controlled recombination. *J. Chem. Phys.* 71:1276–1282.
33. Shoup, D., and A. Szabo. 1982. Role of diffusion in ligand binding to macromolecules and cell-bound receptors. *Biophys. J.* 40:33–39.
34. Mozumder, A. 1982. Mean recombination time of diffusion controlled geminate reactions. *J. Chem. Phys.* 76:5107–5111.
35. Pólya, G. 1921. Über eine Aufgabe der Wahrscheinlichkeitsrechnung betreffend die Irrfahrt im Strassennetz. *Math. Ann. (Berl.).* 84:149–160.
36. Sano, H., and M. Tachiya. 1981. Theory of diffusion-controlled reactions on spherical surfaces and its application to reactions on micellar surfaces. *J. Chem. Phys.* 75:2870–2878.
37. Halle, B., H. Wennerström, and L. Piculell. 1984. Interpretation of counterion spin relaxation in polyelectrolyte solutions. *J. Phys. Chem.* In press.